

Syntheses and Structures of Asymmetric Bis(silyl) Niobocene Hydrides

Konstantin Yu. Dorogov,[†] Muhammed Yousufuddin,[‡] Nam-Nhat Ho,[‡] Andrei V. Churakov,[§] Lyudmila G. Kuzmina,[§] Arthur J. Schultz,^{||} Sax A. Mason,[⊥] Judith A. K. Howard,[#] Dmitry A. Lemenovskii,[†] Robert Bau,^{*‡} and Georgii I. Nikonov^{*†,‡,‡}

Chemistry Department, Moscow State University, Vorob'evy Gory, 119992 Moscow, Russia, Chemistry Department, University of Southern California, Los Angeles, California 90089, Institute of General and Inorganic Chemistry RAS, Leninskii Prosp. 31, 119991 Moscow, Russia, Intense Pulsed Neutron Source, Argonne National Laboratory, Argonne, Illinois 60439, Institut Laue Langevin, Grenoble, France, Chemistry Department, University of Durham, South Road, Durham DH1 3LE, United Kingdom, and Chemistry Department, Brock University, 500 Glenridge Avenue, Saint Catharines, L2S 3A1 Ontario, Canada

Received July 16, 2006

This paper deals with the preparation and structural investigation of asymmetric bis(silyl) niobocene hydrides, Cp₂-Nb(SiHMe₂)(H)(SiXMe₂) (**2**; X = F (**a**), Cl (**b**), Br (**c**), I (**d**)) and Cp₂Nb(SiXMe₂)(H)(SiYMe₂) (X, Y = F–I; X ≠ Y). Complexes **2a–d** were prepared by selective electrophilic activation of the Si–H bond in Cp₂Nb(SiHMe₂)₂(H). The Cp₂Nb(SiXMe₂)(H)(SiYMe₂) complexes were prepared by electrophilic activation of the Si–H bond in **2a–d** and, in some cases, by electrophilic exchange of the X halides in Cp₂Nb(SiXMe₂)₂(H) (**1**) for other halides, Y. The structures of complexes **2b** and **2c** have been studied by X-ray and neutron diffraction (ND). The ND results unequivocally established that the hydride ligand in **2c** is shifted toward the SiBrMe₂ ligand and that in **2b** is positioned symmetrically between two nonequivalent silyl groups, with the H⋯SiCIME₂ distance being shorter because of the shorter Nb–SiCIME₂ bond length. Analysis of the X-ray structures of complexes **2a–d** and complexes Cp₂Nb(SiXMe₂)(H)(SiYMe₂) shows that the largest structural distortions are observed for the silyl groups substituted by heavy halogen atoms. These trends are rationalized in terms of stronger interligand hypervalent interactions (IHI) Nb–H⋯Si–X for heavy atoms X from Group 7.

Introduction

The X-ray and neutron diffraction structures of compound Cp₂Nb(SiCIME₂)₂(H) (**1b**) exhibit unusual structural distortions, which were explained using the concept of interligand hypervalent interactions (IHI).^{1,2} The IHI was suggested to emerge as result of electron-density transfer from the basic

M–H bond of an early transition metal hydride on the antibonding orbital σ*(Si–X) of a functionalized silyl ligand, SiXR₂, resulting in structural and spectroscopic features different from those observed in silane σ-complexes (Figure 1). Such a model also implies a distinctive stereochemical criterion for IHI, namely, the hydride and substituent X at silicon should be in an approximate trans configuration. A very similar interaction between a Ta–H bond and the β-silyl group of a silylamido ligand was observed by Gountchev and Tilley.³ Subsequent research in this area has been focused on the elucidation of the effect of substituents at silicon,⁴ the influence of the metal,⁵ the variation of the ligand environment,⁵ and the identification and further specification

* To whom correspondence should be addressed. E-mail address: gnikonov@brocku.ca (G.I.N.); bau@almaak.usc.edu (R.B.).

[†] Moscow State University.

[‡] University of Southern California Los Angeles.

[§] Institute of General and Inorganic Chemistry RAS.

^{||} Argonne National Laboratory.

[⊥] Institut Laue Langevin.

[#] University of Durham.

[‡] Brock University.

- (1) (a) Nikonov, G. I.; Kuzmina, L. G.; Lemenovskii, D. A.; Kotov, V. *J. Am. Chem. Soc.* **1995**, *117*, 10133. (b) Nikonov, G. I.; Kuzmina, L. G.; Lemenovskii, D. A.; Kotov, V. *J. Am. Chem. Soc.* **1996**, *118*, 6333 (corr).
(2) Bakhmutov, V. I.; Howard, J. A. K.; Keen, D. A.; Kuzmina, L. G.; Leech, M. A.; Nikonov, G. I.; Vorontsov, E. V.; Wilson, C. C. *J. Chem. Soc., Dalton Trans.* **2000**, 1631.

- (3) Gountchev, T. I.; Tilley, T. D. *J. Am. Chem. Soc.* **1997**, *119*, 12831.

- (4) (a) Nikonov, G. I.; Kuzmina, L. G.; Vyboishchikov, S. F.; Lemenovskii, D. A.; Howard, J. A. K. *Chem.—Eur. J.* **1999**, *5*, 2497. (b) Nikonov, G. I.; Kuzmina, L. G.; Howard, J. A. K. *J. Chem. Soc., Dalton Trans.* **2002**, 3037. (c) Dorogov, K. Yu.; Churakov, A. V.; Kuzmina, L. G.; Howard, J. A. K.; Nikonov, G. I. *Eur. J. Inorg. Chem.* **2004**, 771.

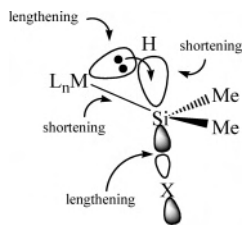


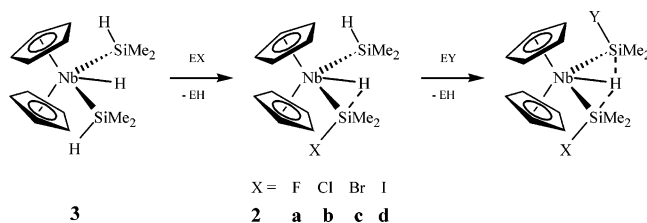
Figure 1.

of structural^{2–4} and spectroscopic features^{5b,c} of IHL. Interactions between one hydride ligand and one silyl ligands (3c–4e interligand interaction)^{4,5} and between one hydride and two silyl groups (5c–6e interligand interaction)^{1,2,4} have been found.⁶

By analogy with hypervalent organosilicon compounds,⁷ it has been assumed that heavier halogen substituents at silicon would give rise to larger structural distortions.^{4a} On the other hand, lighter and more electronegative halogens appear to form stronger Si–X bonds. For example, the stability of species $[\text{SiX}_6]^{2-}$ falls drastically as X descends Group 7.⁸ One can expect that the ionic contribution should be important for the most electron-withdrawing element, fluorine, whereas covalent interaction should dominate for the more polarizable bromine and iodine substituents. Therefore, the effect of the halogen substituent on the extent of Si–H interligand bonding is not straightforward. To attack this problem, we set out to investigate the class of asymmetric complexes $\text{Cp}_2\text{Nb}(\text{SiYMe}_2)(\text{H})(\text{SiXMe}_2)$. We anticipated that nonequivalent silyl groups would compete for the interactions with the central hydride, which should have its manifestation in the structural properties. This assumption gives rise to two important points: (i) systematic structural studies should be carried out, and (ii) ND studies should be performed at least for several compounds of this series to establish unequivocally the asymmetric, if any, position of the hydride. In our previous ND study of the compound **1b**, the hydride was found to be located symmetrically between two identical chlorosilyl groups.²

In this paper, we report syntheses and systematic X-ray investigations of complexes $\text{Cp}_2\text{Nb}(\text{SiYMe}_2)(\text{H})(\text{SiXMe}_2)$ and the neutron diffraction studies of complexes $\text{Cp}_2\text{Nb}(\text{SiHMe}_2)(\text{H})(\text{SiClMe}_2)$ (**2b**) and $\text{Cp}_2\text{Nb}(\text{SiHMe}_2)(\text{H})(\text{SiBrMe}_2)$ (**2c**). A preliminary communication has appeared.⁹

Scheme 1. Synthetic Strategy to Asymmetric Bis(silyl)niobocenes via Selective Si–H Activation



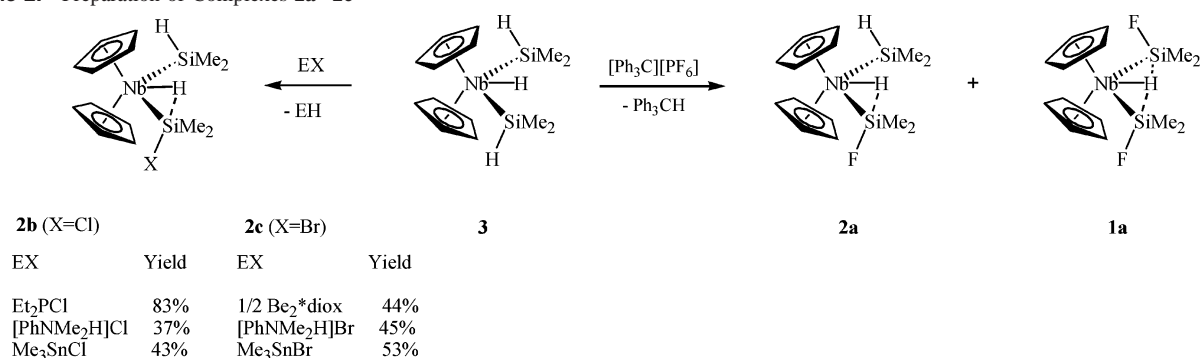
Results and Discussion

Synthetic Strategy. Investigation of the asymmetric $\text{Cp}_2\text{Nb}(\text{SiYMe}_2)(\text{H})(\text{SiXMe}_2)$ complexes faces a tricky problem of defining an effective synthetic strategy toward this class of complexes. The most common method of preparing silyl derivatives, the oxidative addition of the Si–H bonds and salt elimination reactions,¹⁰ is not usually selective, and there are only few reports on the silyl complexes featuring two different silyl ligands.¹¹ In our previous study of symmetrical $\text{Cp}_2\text{Nb}(\text{SiXMe}_2)_2(\text{H})$ compounds, we established several effective routes to functionalized silyl complexes, based on electrophilic activation of the Si–H bond of the compound $\text{Cp}_2\text{Nb}(\text{SiHMe}_2)_2(\text{H})$ (**3**).^{4a,b} If such an activation could be done selectively to give the asymmetric $\text{Cp}_2\text{Nb}(\text{SiHMe}_2)(\text{H})(\text{SiXMe}_2)$ (**2**) complexes in the first step, then a powerful synthetic method for the preparation of the target $\text{Cp}_2\text{Nb}(\text{SiYMe}_2)(\text{H})(\text{SiXMe}_2)$ complexes would be developed (Scheme 1). To the best of our knowledge, selective Si–H activation in transition metal silyl complexes has not been yet investigated.¹² In the following discussion, we shall first consider preparation of mono(halogenated) compounds **2** and then their application to the synthesis of doubly functionalized complexes $\text{Cp}_2\text{Nb}(\text{SiYMe}_2)(\text{H})(\text{SiXMe}_2)$ (X, Y = F–I; X ≠ Y). After that, we shall discuss the structural and NMR features of these new compounds.

Syntheses. Monofluorination of 3. Selective substitution of only one Si–H hydride for a fluoro group turned out to be the most difficult stage of this study. A variety of reagents and conditions have been tried (1/3 $[\text{CPh}_3][\text{PF}_6]$, 1/4 $[\text{CPh}_3][\text{BF}_4]$, 1/3 $\text{F}_3\text{B}\cdot\text{Et}_2\text{O}$, NH_4F , FSnMe_3 , KHF_2) but generally speaking, the selectivity of fluorination was very low. As a rule, a significant amount of the symmetrical complex $\text{Cp}_2\text{Nb}(\text{SiFMe}_2)_2(\text{H})$ (**1a**) was formed, and in some cases, the starting compound **3** was also present. Since all these species

- (5) (a) Nikonov, G. I.; Mountford, P.; Ignatov, S. K.; Green, J. C.; Cooke, P. A.; Leech, M. A.; Kuzmina, L. G.; Razuvaev, A. G.; Rees, N. H.; Blake, A. J.; Howard, J. A. K.; Lemenovskii, D. A. *Dalton Trans.* **2001**, 2903. (b) Ignatov, S. K.; Rees, N. H.; Tyrrell, B. R.; Dubberley, S. R.; Razuvaev, A. G.; Mountford, P.; Nikonov, G. I. *Chem.–Eur. J.* **2004**, *10*, 4991. (c) Dubberley, S. R.; Ignatov, S. K.; Rees, N. H.; Razuvaev, A. G.; Mountford, P.; Nikonov, G. I. *J. Am. Chem. Soc.* **2003**, *125*, 644. (d) Nikonov, G. I.; Mountford, P.; Dubberley, S. R. *Inorg. Chem.* **2003**, *42*, 258. (e) Osipov, A. L.; Gerdov, S. M.; Kuzmina, L. G.; Howard, J. A. K.; Nikonov, G. I. *Organometallics* **2005**, *24*, 587.
- (6) Nikonov, G. I. *Adv. Organomet. Chem.* **2005**, *53*, 217.
- (7) Macharashvili, A. A.; Shklover, V. E.; Struchkov, Yu. T.; Oleneva, G. I.; Kramarova, E. P.; Shipov, A. G.; Baukov, Yu. I. *Chem. Commun.* **1988**, 683.
- (8) Corriu, R. J. P.; Young, C. J. in *The Chemistry of Organosilicon Compounds*; Patai, S., Rappoport, Z., Eds.; Wiley: New York, 1989; 1241.

- (9) Dorogov, K. Yu.; Dumont, E.; Ho, N.-N.; Churakov, A. V.; Kuzmina, L. G.; Poblet, J.-M.; Schultz, A. J.; Howard, J. A. K.; Bau, R.; Lledos, A.; Nikonov, G. I. *Organometallics* **2004**, *23*, 2845.
- (10) (a) Tilley, T. D. In *The Chemistry of Organosilicon Compounds*; Patai, S., Rappoport, Z., Eds.; Wiley: New York, 1989; Chapter 24. (b) Corey, J. Y.; Braddock-Wilking, J. *Chem. Rev.* **1999**, *99*, 175.
- (11) (a) Koloski, T. S.; Pestana, D. C.; Berry, D. H. *Organometallics* **1994**, *13*, 4173. (b) Koloski, T. S.; Pestana, D. C.; Carrol, P. J.; Berry, D. H. *Organometallics* **1994**, *13*, 489. (c) Qiu, H.; Cai, H.; Woods, J. B.; Wu, Z.; Chen, T.; Yu, X.; Xue, Z. *Organometallics* **2005**, *24*, 4190.
- (12) For some related work on silyl functionalization, see: (a) Schubert, U.; Wörle, B.; Jandik, P. *Angew. Chem., Int. Ed. Engl.* **1981**, *20*, 695. (b) Malisch, W.; Jehle, H.; Möller, S.; Thum, G.; Reising, J.; Gbureck, A.; Nagel, V.; Fickert, C.; Kiefer, W.; Nieger, M. *Eur. J. Inorg. Chem.* **1999**, 1597. (c) Malisch, W.; Jehle, H.; Möller, S.; Saha-Möller, K.; Adam, W. *Eur. J. Inorg. Chem.* **1998**, 1585. (d) Thum, G.; Malisch, W. *J. Organomet. Chem.* **1984**, *264*, C5. (e) Wekel, H.-U.; Malisch, W. *J. Organomet. Chem.* **1984**, *264*, C10.

Scheme 2. Preparation of Complexes **2a–2c**

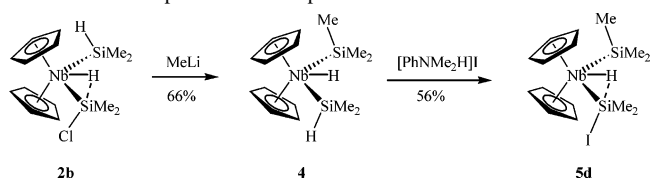
have comparable solubility, the isolation of pure **2a** was very complicated. All three B–F bonds of BF₃ are active but the selectivity is low (1:1:3 ratio of **3/1a/2a** by NMR). The variation of reaction conditions (temperature, solvent) or addition of amine NEt₃ does not improve the selectivity. The literature compound FSnMe₃¹³ fluorinates only one Si–H bond of Cp₂Nb(SiHMe₂)₂(H). Unfortunately, this material also contains a significant amount of ClSnMe₃ (up to 10%), which affects the competitive chlorination of **3**. In contrast, very pure polymeric (FSnMe₃)_n is not active at all. We believe that it is the weak linkage F–Me₂Sn···Cl–SnMe₂ in the polymer chain of (FSnMe₃)_n(ClSnMe₃)_m which gives rise to a reactive center. NH₄F and KHF₂ were inactive in this reaction.

The best result was eventually achieved with a 1/3 equiv of the trityl compound [Ph₃C][PF₆], affording a mixture of mono- and bis(fluorinated) complexes **2a** and **1a**, respectively, in the ratio 1:2 (Scheme 2). Multiple recrystallization from ether afforded analytically pure **2a** in a 27% yield.

As an alternative approach to **2a**, we investigated nucleophilic halogen substitution in the monohalide derivatives Cp₂Nb(SiHMe₂)₂(H)(SiXMe₂) (X = Cl (**2b**), I (**2d**), vide infra). Attempted fluorination with NEt₄F·2H₂O afforded a mixture of the starting compound (**2b** or **2d**), Cp₂NbH₃, and **2a** in a ratio of 1:1:2, which complicated the isolation of the target product. Surprisingly, when Cp₂Nb(SiHMe₂)₂(H)(SiClMe₂) (**2b**) was reacted with CsF, the only observable product formed, in addition to the starting compound, was Cp₂Nb(SiClMe₂)₂(H) (**1b**). Evolution of a noncondensable gas, believed to be dihydrogen, was also observed during the reaction. The mechanistic aspect of this redistribution reaction and the fate of another equivalent of the presumed niobocene product remain unclear.

Monochlorination of 3. Selective monochlorination of **3** to give **2b** can be affected by several reagents, as summarized in Scheme 2. In the case of ClPEt₂, 2 equiv of chlorophosphine are required because 1 equiv is consumed by the initial phosphorus product HPEt₂ to give [Et₂PH → PEt₂]Cl. In all three cases, the reactions occur under mild conditions within a few hours. The undesired bis(chloro) complex **1b** is not formed in any significant amount.

Interestingly, the result of the reaction between **3** and ClSnMe₃ crucially depends on the solvent employed. In ether, the main product is the target **2b**, whereas in toluene, a severe decomposition occurs, and the main soluble product is the

Scheme 3. Preparation of Complexes **4** and **5d**

known compound Cp₂Nb(SiMe₃)₂H (11%).¹⁴ The fate of tin coproducts of this unusual reaction and its mechanism remain unknown.

Monobromination of 3. Complex Cp₂Nb(SiHMe₂)₂(H)(SiBrMe₂) (**2c**) can be conveniently obtained by selective bromination of **3** under the action of 1/2 equiv of Br₂·diox (yield 44%), 2 equiv of BrSnMe₃ (53%), or 1 equiv of [PhNMMe₂]Br (45%, Scheme 2). Compound **2c** is a useful starting material for the preparation of the Br-substituted series Cp₂Nb(SiXMe₂)₂(H)(SiBrMe₂) (X = F, Cl, I) (vide infra).

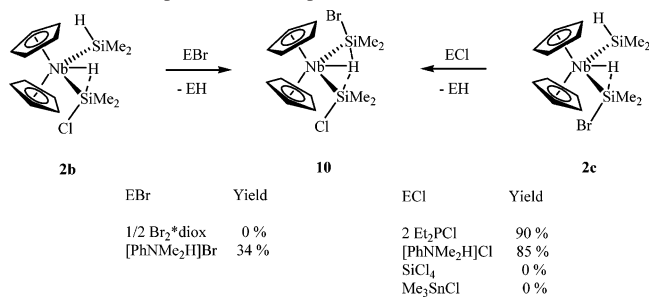
Monoiodination of 3. Reagents I₂, IMe, ISiMe₃, ISnMe₃, and [PhNMMe₂]I have been screened for selective monoiodination. The best result was achieved with the ammonium salt, which allowed for the preparation of **2d** in a 35% isolated yield. The relatively low yield is the result of the side-reaction of the product with the solvent, diethyl ether. Although this problem does not exist in aromatic solvents, the reaction in Et₂O goes faster. Therefore, the isolation of the product should be done immediately upon completion of the reaction (a few hours in ether). Fortunately, **2d** like **1d** is sparingly soluble both in Et₂O and toluene, allowing for its easy isolation from the more soluble byproducts.

When 1/2 equiv of I₂ is used, a difficult-to-separate mixture of **2d** and **1d** (along with **3**) emerges. The presence of 5 equiv of NEt₃ in the reaction does not solve this problem. The reaction of **3** with IMe in ether is violent and leads to complete decomposition of **3** but a very low yield of **2d**. In contrast, in benzene, the reaction is both sluggish and not selective: 30% conversion was achieved only in a year to give a mixture of **2d** and **1d**. ISiMe₃ is more reactive under these conditions (half conversion in benzene at room temperature was achieved in a week) but still not selective.

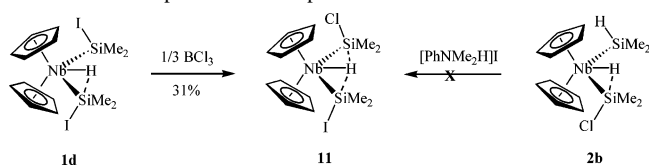
(13) (a) Herzog, A.; Liu, F.-Q.; Roesky, H. W.; Demsar, A.; Keller, K.; Noltenmeyer, M.; Pauer, F. *Organometallics* **1994**, *13*, 1257. (b) Murphy, E. F.; Yu, P.; Dietrich, S.; Roesky, H. W.; Parsini, E.; Noltenmeyer, M. *Dalton Trans.* **1996**, 1983.

(14) Green, M. L. H.; Hughes, A. K. *J. Organomet. Chem.* **1996**, *506*, 221.

Scheme 4. Preparation of Complex 10

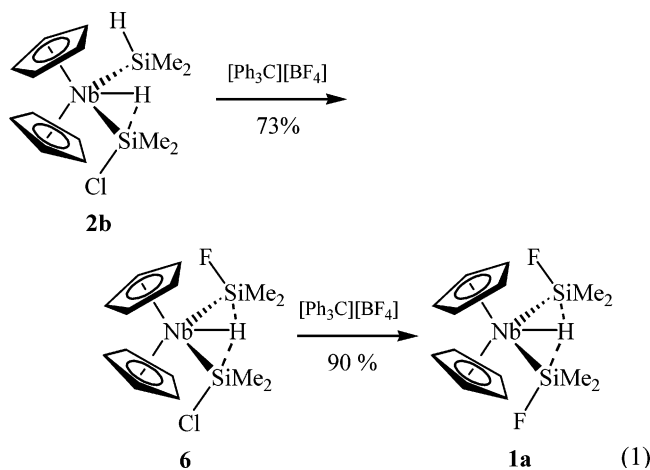


Scheme 5. Preparation of Complex 11



The reaction of **3** with ISnMe_3 in toluene is facile but gives, unexpectedly, the *mono(alkylation)* product $\text{Cp}_2\text{Nb}(\text{SiMe}_3)(\text{H})(\text{SiHMe}_2)$ (**4**). Compound **4** was independently prepared by the reaction of **2b** with MeLi (66%, Scheme 3). Like **3**, this compound reacts violently with air (pyrophoric in the form of fine powder). At the moment, we have no rationale for this reaction and are curious why in toluene ISnMe_3 results in the *mono(alkylation)* of **3**, whereas the related compound ClSnMe_3 gives $\text{Cp}_2\text{Nb}(\text{SiMe}_3)_2(\text{H})$ (vide supra). The reaction of **4** with $[\text{PhNHMe}_2]\text{I}$ gives the *mono(iodo)* derivative $\text{Cp}_2\text{Nb}(\text{SiMe}_3)(\text{H})(\text{SiIme}_2)$ (**5d**), isolated in a 56% yield (Scheme 3).

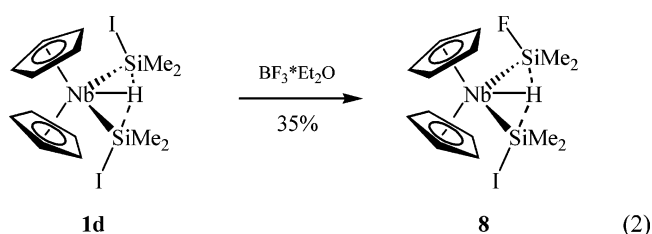
Fluorosubstituted Complexes $\text{Cp}_2\text{Nb}(\text{SiFMe}_2)(\text{H})(\text{SiXMe}_2)$ ($\text{X} = \text{Cl, Br, I}$). Because the *mono(fluoride)* **2a** is not readily accessible, the preparation of the F derivatives $\text{Cp}_2\text{Nb}(\text{SiFMe}_2)(\text{H})(\text{SiXMe}_2)$ ($\text{X} = \text{Cl, Br, I}$) was achieved by the fluorination of $\text{Cp}_2\text{Nb}(\text{SiHMe}_2)(\text{H})(\text{SiXMe}_2)$ ($\text{X} = \text{Cl, Br, I}$). The Cl derivative $\text{Cp}_2\text{Nb}(\text{SiFMe}_2)(\text{H})(\text{SiClMe}_2)$ (**6**) can be easily prepared in a 73% isolated yield by the reaction of **2b** with 1 equiv of $[\text{Ph}_3\text{C}][\text{BF}_4]$ in THF. The Si–Cl bond turned out to be reactive to the trityl cation too, so that the application of 2 equiv of $[\text{Ph}_3\text{C}][\text{BF}_4]$ leads to the difluoride **1a** (eq 1).



Analogously, the reaction of $\text{Cp}_2\text{Nb}(\text{SiBrMe}_2)(\text{H})(\text{SiHMe}_2)$ (**2c**) with $[\text{Ph}_3\text{C}][\text{BF}_4]$ in THF affords the mixed Br/F-

substituted complex $\text{Cp}_2\text{Nb}(\text{SiBrMe}_2)(\text{H})(\text{SiFMe}_2)$ (**7**, 72%). The difluoride **1a** was also observed in a small amount. The latter product most likely emerges as a result of the attack of evolving F_3B on the Si–Br bond. Such a complication has not been observed for **2b**, most likely, because the Si–Cl bond is stronger than the Si–Br bond. Electrophilic fluorination of **1c** by F_3B does occur, but it is a less convenient method of making **7** because the reaction is slower (5:1 mixture of **7** and **1c** was observed after 3 days). Analogous Cl/F exchange in the dichloride **1b** does not occur over an extended period of time.

For an even better leaving group, iodine, the I/F exchange in **1d** is a practical method to prepare the asymmetric complex $\text{Cp}_2\text{Nb}(\text{SiIme}_2)(\text{H})(\text{SiFMe}_2)$ (**8**) (eq 2). Thus, the 1:1 reaction of $\text{Cp}_2\text{Nb}(\text{SiIme}_2)_2(\text{H})$ (**1d**) with $\text{F}_3\text{B}\cdot\text{Et}_2\text{O}$ in toluene affords **8** in a 35% isolated yield. It is interesting that, although the initially formed product, $\text{IF}_2\text{B}\cdot\text{Et}_2\text{O}$, could be expected to be a more-active fluorinating agent (because of its increased Lewis acidity),¹⁵ only one Si–I bond of **1d** is touched. We explain this controversy in terms of facile iodination of the ether part of the adduct $\text{IF}_2\text{B}\cdot\text{Et}_2\text{O}$ to give the less-acidic $(\text{EtO})_2\text{F}_2\text{B}$. The isolation of slightly soluble **8** by recrystallization from the unreacted and also slightly soluble **1d** has been achieved only after ultrasonication of the mixture. In light of this, it is not surprising that the reaction of **1d** and $\text{F}_3\text{B}\cdot\text{Et}_2\text{O}$ in THF gives the fluoro-alkoxide derivative $\text{Cp}_2\text{Nb}(\text{Si}(\text{O}(\text{CH}_2)_4\text{I})\text{Me}_2)(\text{H})(\text{SiFMe}_2)$ (**9**), the product of ring opening in the THF. The attachment of the fluoro group to the SiMe_2 moiety rather than to the butylidene fragment follows from the observation of an H–F coupling constant for the methyl group signal in the ^1H NMR spectrum, $J(\text{H}-\text{F}) = 8$ Hz. The same pattern is observed for all other complexes featuring the SiFMe_2 group.



Attempted chlorine substitution in the compound $\text{Cp}_2\text{Nb}(\text{SiFMe}_2)(\text{H})(\text{SiClMe}_2)$ (**6**) by ISiMe_3 in ether resulted in decomposition.

Chlorosubstituted Complexes $\text{Cp}_2\text{Nb}(\text{SiClMe}_2)(\text{H})(\text{SiXMe}_2)$ ($\text{X} = \text{Br, I}$). The compound $\text{Cp}_2\text{Nb}(\text{SiClMe}_2)(\text{H})(\text{SiBrMe}_2)$ (**10**) can be obtained either by the chlorination of **2c** or by the bromination of **2b**, both starting materials being readily available through the selective halogenation of **3** (Scheme 4). Chlorination of **2c** by ClPEt_2 or by $[\text{PhNHMe}_2]\text{Cl}$ gives **10** in high yield. Bromination of **2b** by $[\text{PhNHMe}_2]\text{Br}$ affords **10** in a 34% yield. Other reagents tested in these reactions, $\text{Br}_2\cdot\text{dioxane}$, Cl_4Si , and ClSnMe_3 , were not effective.

(15) Mingos, D. M. P. *Essential Trends in Inorganic Chemistry*; Oxford University Press: Oxford, U.K., 1998.

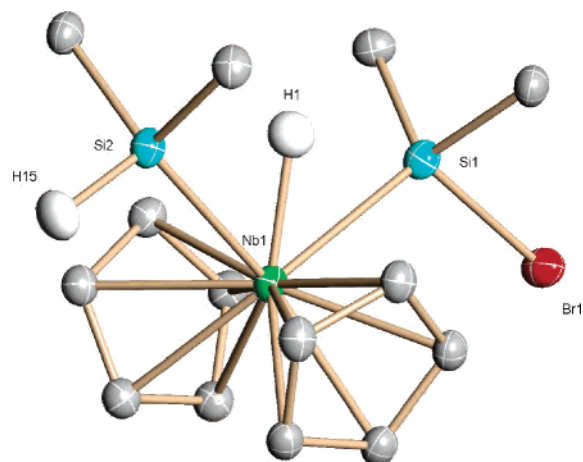


Figure 2. Molecular structure of complex $\text{Cp}_2\text{Nb}(\text{SiHMe}_2)(\text{H})(\text{SiBrMe}_2)$ (**2c**) as obtained from the neutron diffraction analysis (thermal ellipsoids are plotted at 50% probability). For the view of the structure of related complex **2b**, see ref 9.

Table 1. Selected Bond Distances (Å) and Bond Angles (deg) in Complexes $\text{Cp}_2\text{Nb}(\text{SiHMe}_2)(\text{H})(\text{SiClMe}_2)$ (**2b**), $\text{Cp}_2\text{Nb}(\text{SiHMe}_2)(\text{H})(\text{SiBrMe}_2)$ (**2c**), and $\text{Cp}_2\text{Nb}(\text{SiClMe}_2)_2(\text{H})$ (**1b**) Determined by Neutron Diffraction

	2b ^a	2c	1b
Nb–H	1.80(2)	1.80(1)	1.816(8)
XSi···H	2.09(2)	2.06(1)	2.076(3)
HSi···H	2.13(2)	2.19(1)	-
XSi(2)–Nb–H	52.9(6)	52.1(3)	52.14(5)
HSi(1)–Nb–H	52.9(6)	55.0(3)	-
Si–H	1.461(10)	1.54(1)	-

^a Combined neutron diffraction/X-ray study.

$\text{Cp}_2\text{Nb}(\text{SiClMe}_2)(\text{H})(\text{SiMe}_2)$ (**11**) can be conveniently prepared by the Cl/I exchange reaction of **1d** with a $1/3$ equiv of Cl_3B (yield 31%, Scheme 5). Attempted iodination of **2b** by $[\text{PhNHMe}_2]\text{I}$ in ether resulted in a mixture of iodo- and chloro-substituted complexes which was difficult to separate.

Preparation of $\text{Cp}_2\text{Nb}(\text{SiBrMe}_2)(\text{H})(\text{SiMe}_2)$ (12**).** The last asymmetric complex from this series, the Br/I derivative $\text{Cp}_2\text{Nb}(\text{SiBrMe}_2)(\text{H})(\text{SiMe}_2)\text{H}$ (**12**) was obtained by the treatment of **2c** with iodine (24% isolated yield). The bromination of **2d** by Br_2 -dioxane afforded a mixture of Br- and I-substituted complexes, which was difficult to separate.

Neutron Diffraction Studies. The molecular structures of two related mono(halogen)-substituted complexes, $\text{Cp}_2\text{Nb}(\text{SiClMe}_2)(\text{H})(\text{SiHMe}_2)$ ⁹ (**2b**) and $\text{Cp}_2\text{Nb}(\text{SiBrMe}_2)(\text{H})(\text{SiHMe}_2)$ (**2c**, Figure 2), have been determined by neutron diffraction. Their selected molecular parameters are given in Table 1. In the structure of **2b**, the hydride occupies the exact central position between two lateral silyl groups, both Si–Nb–H bond angles being equal to 52.9(6)°. The same situation has been previously observed in the ND structure of symmetrical complex $\text{Cp}_2\text{Nb}(\text{SiClMe}_2)_2(\text{H})$ (**1b**).^{4b} However, because the Nb–SiCl bond length is shorter than the Nb–SiH bond length (2.5969(6) and 2.6522(6) Å, respectively), the hydride appears to lie closer to the SiClMe₂ group than to the SiHMe₂ ligand (2.085(17) vs 2.126(17) Å). The former value compares well with the related distance observed by ND in compound **1b** with IHI (2.076(3) Å).^{4b}

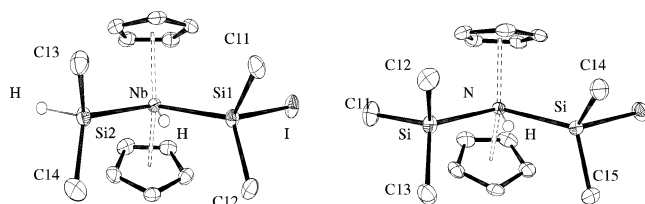


Figure 3. Molecular structures of complexes **2d** and **5d**. The X-ray structure of other mono(halogen)-substituted complexes (**2a–c**) are similar and are given in Supporting Information.

The Nb–H bond length of 1.804(17) Å is also close to the ND value of 1.816(8) Å determined in **1b**^{6b}. Other Group 5 metallocene hydrides studied by neutron diffraction have somewhat shorter M–H bonds, that is, 1.785(15) Å in $\text{Cp}_2\text{Ta}(\text{SiHMe}_2)_2(\text{H})$ ¹⁶ and 1.771(9) Å (av) in Cp_2TaH_3 .¹⁷ Note that the atomic radii of Nb and Ta are almost identical (1.429 and 1.43 Å),¹⁸ so that the comparison of M–H bond lengths in these systems is fair. Decreased H–Si contacts and elongated M–H bonds are characteristic features of interligand hypervalent interactions between the silyl and hydride ligands.^{4–6}

In contrast, the ND study of the bromine analog of **2b**, the compound $\text{Cp}_2\text{Nb}(\text{SiBrMe}_2)(\text{H})(\text{SiHMe}_2)$ (**2c**, Table 1), exhibits a clear shift of the hydride ligand to the bromosilyl ligand. This is seen both from the smaller BrSi–Nb–H bond angle (52.1(3) vs 55.0(3)° for HSi–Nb–H) and from much larger difference in the Si–H (hydride) distances (2.06(1) Å for the BrSi–H contact vs 2.19(1) Å for the HSi–H distance). Meanwhile, the Nb–H bond length of 1.80(1) Å remains almost the same as in **2b**. This hydride shift to the SiBrMe₂ group is statistically meaningful, and there is no obvious steric reason for such a shift. Moreover, the electronic structure of trisubstituted niobocenes dictates that the central ligand occupied the central position in the metallocene bisecting plane where it finds the best overlap with the frontier orbital of the bent Cp_2M fragment.¹⁹ In fact, in **2c**, the hydride deviates from this central position defined by the Cent1–Nb–Cent2 plane (Cent stands for the centroid of the Cp ring) by 0.053 Å, a feature absent in **2b**. Such a deviation should result in the decrease of M–H bonding,^{19a} likely at the expense of forming a H–Si interaction. To conclude, this hydride shift unequivocally establishes a stronger interaction of the hydride with the SiBrMe₂ ligand.

Other molecular parameters of complexes **2b** and **2c** are discussed in the next section.

X-ray Studies of Monohalo-Substituted Complexes 2a–d and 5d. In this work, we performed five X-ray diffraction studies of asymmetric mono(halogen) substituted (**2a–d** and **5d**, Figure 3) and five X-ray diffraction studies of asymmetric dihalogen-substituted bis(silyl) niobocene complexes (**6–8**, **10**, and **12**, Figure 4). We failed to grow

(16) Tanaka, I.; Ohhara, T.; Nimura, N.; Ohashi, Y.; Jiang, Q.; Berry, D. H.; Bau, R. *J. Chem. Res.* **1999**, 14.

(17) Wilson, R. D.; Koetzle, T. F.; Hart, D. W.; Kvick, A.; Tipton, D. L.; Bau, R. *J. Am. Chem. Soc.* **1977**, *99*, 1775.

(18) Emsley, J. *The Elements*, 2nd ed.; Clarendon Press: Oxford, U.K., 1991.

(19) (a) Lauher, J. W.; Hoffmann, R. *J. Am. Chem. Soc.* **1976**, *98*, 1729. (b) Green, J. C. *Chem. Soc. Rev.* **1998**, 263.

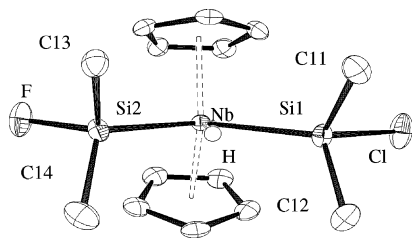


Figure 4. Molecular structures of **6**. Molecular structures of other bis-(halogen)-substituted complexes (**7**, **8**, **10**, and **12**) are similar and are given in Supporting Information.

an X-ray quality crystal of the compound $\text{Cp}_2\text{Nb}(\text{SiClMe}_2)(\text{H})(\text{SiIme}_2)$ (**11**), the only missing member of this series. The X-ray structures of compounds $\text{Cp}_2\text{Nb}(\text{SiFMe}_2)(\text{H})(\text{SiHMe}_2)$ (**2a**), $\text{Cp}_2\text{Nb}(\text{SiClMe}_2)(\text{H})(\text{SiBrMe}_2)$ (**10**), and $\text{Cp}_2\text{Nb}(\text{SiBrMe}_2)(\text{H})(\text{SiIme}_2)$ (**12**) are disordered in the positions of non-methyl substituents at the silicon atoms (i.e., the F and H in **2a**, Cl and Br in **10**, and Br and I in **12**). This disorder mixes up the observed Nb–Si and Si–X distances, the molecular parameters of crucial importance for our discussion, so that it is not possible to discuss the competitive interligand interactions in these complexes. The compounds **2b** and **2c** exhibit a rotational disorder of the SiHMe_2 fragment which does not affect the analysis of IHI in the latter systems.

All ten X-ray structures of compounds $\text{Cp}_2\text{Nb}(\text{SiXMe}_2)(\text{H})(\text{SiYMe}_2)$ under discussion exhibit the same structural feature, namely, regardless the size of the halide substituent at silicon, the halogen atom is located in the bisecting plane of the niobocene fragment trans to the hydride (Figure 3). Such a geometry, also observed in the symmetrical compounds **1a–d**, is sterically favorable for X, Y = Br and I but not for the smaller fluorine substituent. This sterically unfavorable trans H–Si–H geometry is also observed for the SiHMe_2 group of **2a** and **2d** and is also the most populated rotamer for the rotationally disordered complexes **2b** and **2c**. For the latter two compounds, this kind of disorder suggests that the difference in energy of two conformers, stemming from the difference in the steric interaction Cp– SiHMe_2 , is comparable to the energy of weak interligand interaction Nb–H \cdots Si–H.

Another feature amenable to all these compounds is the markedly decreased Si–Nb–Si bond angles (range 105.85–(2)–107.99(2) $^\circ$) compared to what is found for the related classical bis(silyl) hydride metallocenes of the Group 5 metals (range = 109.61(2)–110.81(5) $^\circ$).^{4a,16} Finally, the Si–X bond lengths are elongated and the Nb–Si bonds are shortened relatively classical analogues. All these structural trends are the characteristic signatures of compounds with IHI.⁶

The key molecular parameters of complexes **2a–d** are given in Table 2. The specific conformation of the SiFMe_2 fragment and the diminished Si–Nb–Si bond angle of 106.31(3) $^\circ$ suggest the presence of IHI. This angle is, however, larger than that in the corresponding difluoride $\text{Cp}_2\text{Nb}(\text{SiFMe}_2)_2(\text{H})$ (105.57(4) $^\circ$), which has two attractive FSi \cdots H bonds.^{4a} This difference can be rationalized in terms of stronger FSi \cdots H interaction than the HSi \cdots H interaction. In

Table 2. Selected Bond Distances (Å) and Bond Angles (deg) in Complexes $\text{Cp}_2\text{Nb}(\text{SiHMe}_2)(\text{H})(\text{SiXMe}_2)$ (X = F–I) and $\text{Cp}_2\text{Nb}(\text{SiMe}_3)(\text{H})(\text{SiIme}_2)$ Determined by X-ray Study

	X = F, 2a ^a	X = Cl, 2b	X = Br, 2c	X = I, 2d	X = I, 5d
Nb–Si(X)	2.6411(8)	2.5969(6)	2.586(2)	2.5782(8)	2.5817(7)
Nb–Si(H)	2.6167(8)	2.6522(6)	2.649(2)	2.6426(2)	2.6645(6)
Si–X	1.614(3), 1.581(5)	2.1829(7)	2.377(2)	2.6287(8)	2.6413(6)
(X)Si–Nb–Si	106.31(3)	105.85(2)	107.27(8)	107.99(2)	106.01(2)

^a The SiFMe_2 and SiHMe_2 groups are disordered in the positions of the F and H atoms.

2a, the fluorine and hydrogen positions at silicon are disordered with populations of 0.6/0.4, which is not surprising, taking into account that the van der Waals radii of fluorine and hydrogen are comparable (1.35 and 1.20 Å, respectively).¹⁸ As expected, the silyl group “enriched” with fluorine (population 0.6) exhibits a shorter Nb–Si distance (2.6167(8) vs 2.6411(8) Å) and a longer Si–F distance (1.614(3) vs 1.581(5) Å) than the other silyl group. In the bis(fluoro)-substituted compound **1a** the corresponding parameters were 2.618(1) and 2.622(1) Å for the two Nb–Si bonds and 1.652(3) and 1.644(3) Å for the Si–F bonds.

The molecular structure of **2b** determined by X-ray diffraction exhibits a Si–Cl bond of 2.1829(7) Å (Table 2) elongated compared with that of the previously studied complexes with IHI: $\text{Cp}_2\text{Nb}(\text{SiClMe}_2)_2(\text{H})$ ^{4a} (**1b**, 2.163(1) Å), $\text{Cp}_2\text{Nb}(\text{SiClMe}_2)(\text{H})_2$ ^{4a} (2.170(2) Å), and $\text{Cp}(\text{ArN})\text{Ta}(\text{PMe}_3)(\text{H})(\text{SiClMe}_2)$ ^{5c} (2.177(2) Å). This bond length is among the longest Si–Cl bond length in sterically unencumbered chlorosilyl complexes of transition metals.²⁰ The only other compound with IHI with a longer Si–Cl bond of 2.223–(2) Å is the titanocene complex $\text{Cp}_2\text{Ti}(\text{PMe}_3)(\text{H})(\text{SiCl}_2\text{Me})$.^{5b}

The Si–Br bond length in **2c** is significantly longer than that in $\text{Cp}_2\text{Nb}(\text{SiBrMe}_2)_2(\text{H})$ (2.378(2) vs 2.349(2) Å) and is 11% longer than that in bromosilanes. There are no other structurally characterized mono(bromo)-substituted silyl complexes to underpin the elongation of the Si–Br bond. In fact, this increase of the Si–Br bond length in **2c** relative to **1c** ($\Delta = 0.028(1)$ Å) is more significant than the elongation of the Si–Cl bond in **2b** relative to **1b** ($\Delta = 0.020(1)$ Å). This trend, therefore, is in agreement with the stronger BrSi \cdots H interaction suggested by the neutron diffraction study (vide supra). The strengthening of the BrSi \cdots H interaction is further supported by the contraction of the Nb–SiBrMe₂ bond in **2c** (2.586(2) Å) relative to **1c** (2.604(2) Å). In the comparison of **1b** with **2b**, the localization of IHI on only one silyl center (SiBrMe_2) leads to the opening up of the Si(1)–Nb(1)–Si(2) bond angle from 103.37(7) $^\circ$ in $\text{Cp}_2\text{Nb}(\text{SiBrMe}_2)_2(\text{H})$ to 107.27(7) $^\circ$ in **2b**.

The iodo compounds, **2d** and **5d** (Table 2), are only the second and third examples, respectively, of a transition metal

(20) Bulky groups at silicon in the SiXR_2 group can exert long SiCl bonds even in the absence of any interligand interactions, see: (a) Zarate, E. A.; Kennedy, V. O.; McCune, J. A.; Simons, R. S.; Tessier, C. A. *Organometallics* **1995**, *14*, 1802. (b) Simons, R. S.; Gallicci, J. C.; Tessier, C. A.; Youngs, W. J. *J. Organomet. Chem.* **2002**, *654*, 224. (c) Dorogov, K. Yu.; Churakov, A. V.; Kuzmina, L. G.; Howard, J. A. K.; Nikonov G. I. *Eur. J. Inorg. Chem.* **2004**, 771.

iodosilyl complex, the first one being the symmetrical congener **1d**. The Si–I bonds in **2d** and **5d** are elongated (2.6287(8) and 2.6313(6) Å, respectively) both versus **1d** (2.595(3) Å) and versus the Si–I bonds organosilanes (average 2.537 Å).²¹ This relative elongation of the Si–Hal bond in the iodo derivatives is larger than that observed in the bromo- and chloro-substituted complexes, **2b** and **2c**, respectively, which can be interpreted in terms of enhanced IHI of the hydride with the iodosilyl group. This conclusion is in agreement with the variation of the Nb–Si bonds in the mono(iodo) derivatives. That is, both **2d** and **5d** have shorter Nb–Si bonds (2.5782(8) and 2.5817(7) Å, respectively) than **1d** (2.595(3) Å). Like in other mono(halogen) derivatives discussed above, the Si–Nb–Si bond angles in **2d** and **5d** are increased relative to **1d** (107.99(2) and 106.01(2) vs 104.4(1)°). In accordance with Bent's rule,²² the Nb–SiMe₃ bond of 2.6645(6) Å in **5d** is a longer than the Nb–SiHMe₂ bond of 2.6426(2) Å in **2d**, but it is very close to the Nb–Si bond in the compound Cp₂Nb(CH₂=CH₂)(SiMe₃) (2.669(1) Å).

Systematic Trends in X-ray Structures. Analyzing the variation of structural parameters in the series of mono(halogen) substituted complexes **2a–d** and the compound Cp₂Ta(SiHMe₂)₂(H),^{23,24} one can see that the Nb–Si bond length monotonously decreases from 2.6289(8) Å in **2a** (average of two bonds) to 2.5782(8) Å in **2d**. The Ta–Si bond length in Cp₂Ta(SiHMe₂)₂(H) is closer to the M–Si bonds in the F-substituted complex **2a** rather than to those of the I derivative **2d**, in spite of the big difference in electronegativity of hydrogen (2.20, Pauling)¹⁸ and fluorine (3.98, Pauling).¹⁸ Therefore, the dependence of the Nb–SiX bond length in compounds Cp₂Nb(SiXMe₂)(H)(SiHMe₂) does not follow a simple electronegativity trend and is, thus, at odds with Bent's rule that predicts a monotonous elongation of the M–SiX bond upon decreasing the electronegativity of X.²² In the symmetrical complexes Cp₂Nb(SiXMe₂)₂(H), the Nb–Si bond length goes via a minimum observed for X = Cl.^{4a}

The Si–M–Si bond angle decreases from 110.8(4)° in Cp₂Ta(SiHMe₂)₂(H) to 105.85(2)° **2b**, which corresponds to the decrease of the Si–M–H bond angle from 55.5(5) to 52.9(6)°, and then it increases to 107.99(2)° in compound **2d**. Given the results of the accurate ND study for **2c**, it is justified to say that this opening of the Si–Nb–Si bond angle mainly comes from the increase of HSi–Nb–H bond angle.

Altogether, these results suggest two conclusions: (i) the interligand interactions in the mono(halo)-substituted complexes **2a–d** are increased in comparison with their dihalogen-substituted analogs **1a–d** and (ii) the Nb–H···SiX

Table 3. Selected Molecular Parameters in Complexes Cp₂Nb(SiXMe₂)(H)(SiYMe₂) Determined by X-ray Study (bonds in Å, angles in deg)

	6	7	8	10 ^a	12 ^b
Nb–SiX	2.6206(8) (X = F)	2.625(1) (X = F)	2.6148(9) (X = F)	2.5986(4) (X = Cl)	2.6045(8) (X = Br)
Nb–SiY	2.6038(8) (Y = Cl)	2.594(1) (Y = Br)	2.5837(9) (Y = I)	2.5986(4) (Y = Br)	2.6045(8) (Y = I)
Si–X	1.649(2) (X = F)	1.670(4) (X = F)	1.647(2) (X = F)	2.272(4) (X = Cl)	2.4846(8) (X = Br)
Si–Y	2.180(1) (Y = Cl)	2.369(1) (Y = Br)	2.6173(9) (Y = I)	2.272(4) (Y = Br)	2.4846(8) (Y = I)
XSi–Nb–SiY	105.80(2)	106.32(4)	106.87(3)	103.61(2)	102.64(4)

^a The SiClMe₂ and SiBrMe₂ groups are disordered in the positions of Cl and Br atoms. ^b The SiIMe₂ and SiBrMe₂ groups are disordered in the positions of I and Br atoms.

interaction increases as halogen X descends Group 7, as it was assumed in the previous studies.⁴

X-ray Studies of Asymmetric Dihalogen-Substituted Complexes Cp₂Nb(SiXMe₂)(H)(SiYMe₂) (X, Y = F, Cl, Br, I; X ≠ Y). X-ray structures of complexes **6–8**, **10**, and **12** were performed to determine a *concurrent interligand H–Si interaction* of two different halosilyl groups. All these complexes have the same conformational feature as the related complexes **1a–d** and **2a–d** (namely, the halides X and Y are trans to the hydride) and exhibit decreased Si–Nb–Si bond angles (range of 102.64(4)–106.87(2)°), suggesting that both silyl groups are attracted to the hydride.

In the series of fluoro-complexes Cp₂Nb(SiFMe₂)(H)(SiYMe₂) (Y = F–I and H), the Nb–SiY bond (Tables 2 and 3) decreases down the Group 7 elements in the contradiction with Bent's rule. The Si–Y bonds (Y = Cl–I) are longer than those in the corresponding symmetrical complexes Cp₂Nb(SiXMe₂)₂(H) but are less than the values observed in the mono(halogen)-substituted complexes **2b–d** (for the Si–Cl bond, 2.180(1) Å in **6** vs 2.1829(7) Å in **2b**; for the Si–Br bond, 2.369(1) Å in **7** vs 2.377(2) Å in **2c**; for the Si–I bond, 2.6173(9) Å in **8** vs 2.6287(8) Å in **2c**). In contrast, both the Nb–SiF (range = 2.6148(9)–2.626(1) Å) and the Si–F bond lengths (range = 1.647(2)–1.670(4) Å) compare well with the values observed in **1a** and **2a**. The FSi–Nb–SiY bond angle opens up from Y = F to Y = I, which can be rationalized in terms of decreased FSi···HNb interactions in the presence of a competing SiYMe₂ group. Altogether, these trends suggest that in the presence of a SiYMe₂ ligand (Y ≠ F) the behavior of the SiFMe₂ group resembles very much the behavior of SiHMe₂ group. Heavier halides exert stronger Si···HNb interactions with the silyl ligands to which they are attached.

Analysis of structural parameters in the Cl-substituted complexes Cp₂Nb(SiClMe₂)(H)(SiYMe₂) (Y = F, Br, I and H, Tables 2 and 3) is complicated by the Br/Cl positional disorder in the compound Cp₂Nb(SiClMe₂)(H)(SiBrMe₂) (**10**) and the absence of X-ray structure for the compound Cp₂Nb(SiClMe₂)(H)(SiIMe₂) (**11**). In **10**, the observed averaged Nb–Si bond length of 2.5987(4) Å lies between the values observed in the symmetrical compounds Cp₂Nb(SiMe₂Y)₂(H) (2.597(1) Å in **1b** and 2.604(2) Å in **1c**), the Si–Hal distance is also found between the Si–Cl and Si–Br bond

(21) Average for 5 structures from CCDC, see: Allen, F. H.; Kennard, O. *Chem. Des. Autom. News* **1993**, 8, 31.

(22) Bent, H. A. *Chem. Rev.* **1961**, 61, 275.

(23) The X-ray structure of **3** has not been determined, but the related tantalum complex Cp₂Ta(SiHMe₂)₂H was studied by both X-ray and ND.²⁴ Given the fact that the atomic radii of Nb and Ta are almost identical,¹⁸ it is justified to discuss tantalum derivatives in place of their niobium analogues.

(24) Tanaka, I.; Ohhara, T.; Niimura, N.; Ohashi, Y.; Jiang, Q.; Berry, D. H.; Bau, R. *J. Chem. Res.* **1999**, 14.

lengths observed in **1b** and **1c** (2.163(1) Å in **1b** and 2.349-(2) Å in **1c**). In the series $\text{Cp}_2\text{Nb}(\text{SiClMe}_2)(\text{H})(\text{SiYMe}_2)$, the Si–Cl bond length decreases from Y = H through Y = F to Y = Cl when the Si–Y bond starts to compete effectively with the Si–Cl bond for the interaction with hydride. The only parameter, pertinent to all the compounds from this series, the ClSi–Nb–SiY bond angle, decreases from Y = H to Y = F and then to Y = Br in accordance with strengthening of the H–SiY interactions.

An analogous problem was observed for the series of Br-complexes $\text{Cp}_2\text{Nb}(\text{SiBrMe}_2)(\text{H})(\text{SiYMe}_2)$ (Y = F–I and H, Tables 2 and 3): the compound $\text{Cp}_2\text{Nb}(\text{SiBrMe}_2)(\text{H})(\text{SiMe}_2)$ (**12**) exhibits a Br/I disorder so that two Nb–Si bond lengths, and two Si–Y bond lengths are averaged. The Nb–Br bond length increases monotonously from X = H to X = F and then down Group 7. Accordingly, the Si–Br bond length decreases and the BrSi–Nb–SiY bond angle decreases in the same order. These trends can be again rationalized in terms of increased IHI in the case of heavier halides.

Similar trends are observed for the iodo-series $\text{Cp}_2\text{Nb}(\text{SiI Me}_2)(\text{H})(\text{SiXMe}_2)$ (Y = F, Br, I and H, Tables 2 and 3). The strongest ISi–H interaction is in the compound **2d**, which decreases when the SiMe_2H group is substituted for SiFMe_2 and then decreases further down Group 7 because of the competition of two halosilyl groups for the interaction with the central hydride. The IHI becomes more delocalized (5c–6e), and each individual Si–H interaction gets weaker than in the case of an almost pure 3c–4e IHI in **2d**.

NMR Studies. The measurement of NMR Si–H coupling constants for many years remained the main method to characterize nonclassical Si–H interactions.⁶ Unfortunately, this technique cannot be applied to niobium silyl hydride because of the so-called “quadrupolar broadening”.²⁵ The high-spin niobium nucleus (spin 9/2) causes significant broadening of signals of all magnetically active nuclei (H, P, Si, C, etc.) directly bound to it, thus making the determination of $J(\text{H}–\text{Si})$ practically impossible. However, as we pointed out in the previous report on the symmetrical compounds **1**, other NMR parameters could provide *indirect evidence* for the presence of Si–H interactions.^{4a} For example, the high-field shift of the hydride signal in the ^1H NMR spectrum is a good indicator for the involvement of this hydride in a nonclassical bonding.⁶ It was therefore of interest to establish a correlation, if any, of the NMR parameters of complexes **2**, **6–8**, **10**, and **12** with their structural data.

The ^1H NMR spectra of bis(silyl) complexes $\text{Cp}_2\text{Nb}(\text{SiXMe}_2)(\text{H})(\text{SiYMe}_2)$ (X, Y = H, Hal) exhibit three well-separated groups of signals: the Cp signal (4.36–4.72 ppm), the Me signal (0.29–1.04 ppm), and the hydride signal found in the range from –3.82 to –5.26 ppm. In addition, complexes **2** show the Si–H signal of the SiHMe_2 group at 4.70–5.02 ppm.

All known bis(silyl) hydride complexes of niobium can be classified into three groups, according to the position of

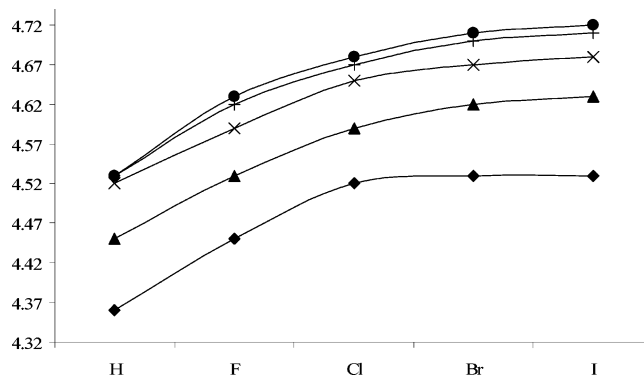


Figure 5. Dependence of the ^1H NMR Cp group signal in complexes $\text{Cp}_2\text{Nb}(\text{SiXMe}_2)(\text{H})(\text{SiYMe}_2)$ on the nature of substituents X and Y: ◆, $\text{Cp}_2\text{Nb}(\text{SiHMe}_2)(\text{H})(\text{SiXMe}_2)$; ▲, $\text{Cp}_2\text{Nb}(\text{SiFMe}_2)(\text{H})(\text{SiXMe}_2)$; ×, $\text{Cp}_2\text{Nb}(\text{SiClMe}_2)(\text{H})(\text{SiXMe}_2)$; +, $\text{Cp}_2\text{Nb}(\text{SiBrMe}_2)(\text{H})(\text{SiXMe}_2)$; ●, $\text{Cp}_2\text{Nb}(\text{SiI Me}_2)(\text{H})(\text{SiXMe}_2)$.

the hydride signals in the ^1H NMR spectra. Group I (–4.9 to –5.4 ppm) is formed by complexes featuring a halogen substituents at each silyl ligand. These complexes have strongly delocalized 5c–6e IHI according to X-ray and ND data. The second group (–4.2 to –4.7 ppm) is formed by compounds with only one halosilyl group, in which the hydride is involved in a stronger but more localized (3c–4e) IHI. The disubstituted complexes $\text{Cp}_2\text{Nb}(\text{Si(SPh)Me}_2)_2(\text{H})$ and $\text{Cp}_2\text{Nb}(\text{Si(PPh}_2\text{)Me}_2)_2(\text{H})$, which according to X-ray studies appear to be virtually classical,^{4b} also signal in this range. Finally, Group III (–3.2 to –3.8 ppm) is composed of compounds with donating alkyl/aryl substituents at silicon, which might be anticipated to have the most hydridic and hence the highest upfield shifted signal for the hydride ligand, but in fact, they exhibit resonances in the lowest field. These complexes are classical. The perchloro-functionalized complex $\text{Cp}_2\text{Nb}(\text{SiCl}_3)_2(\text{H})$, which lacks IHI, is also found here.^{4c}

From simple electronic considerations, one could expect that more electron-withdrawing groups at silicon would cause more downfield shift of the Cp signal. In fact, the data of Figure 5 show that it is the heavier, less electronegative, halogens that exert the most downfield-shifted resonance. For the most-electronegative substituent, fluorine, the Cp signals come closer to the Cp signals of complexes with the most-electropositive substituent X, hydrogen. This trend correlates nicely with the X-ray data that also show that the SiFMe_2 and SiHMe_2 series have rather close structural parameters. It is reasonable to assume that the downfield shift of the Cp signal in the case of Br and I is caused by the more effective electron density transfer from the Cp to the silyl ligand by means of IHI (via the metal hydride) rather than by a simple inductive effect.

This conclusion is further supported by the trends in the Me signals (Figure 6). Again, there is no simple dependence of the position of the signal on the electronegativity of substituents X and Y (the signals of the SiHMe_2 and SiFMe_2 groups are rather close to each other), so that a simple inductive effect is of minor importance. Rather, heavier halogens cause a stronger downfield shift of the Me group signal. The greater the difference between the halogens X

(25) Labinger, J. A. In *Comprehensive Organometallic Chemistry*, Vol. 3; Able, R. W., Wilkinson, G., Stone, F. G. A., Eds.; Pergamon: Elmsford, NY, 1983.

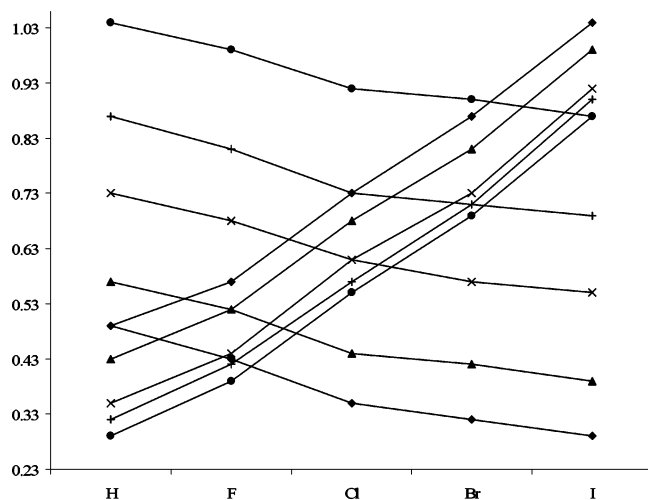


Figure 6. Dependence of the ^1H NMR Me group signal in complexes $\text{Cp}_2\text{Nb}(\text{SiXMe}_2)(\text{H})(\text{SiYMe}_2)$ on the nature of substituents X and Y. The increasing curve stands for X in case of $\text{Cp}_2\text{Nb}(\text{SiXMe}_2)(\text{H})(\text{SiHMe}_2)$ or for the heavier of halogens in case of $\text{Cp}_2\text{Nb}(\text{SiMe}_2\text{X})(\text{SiMe}_2\text{Y})\text{H}$: ■, $\text{Cp}_2\text{Nb}(\text{SiXMe}_2)_2\text{H}$; ◆, $\text{Cp}_2\text{Nb}(\text{SiHMe}_2)(\text{H})(\text{SiXMe}_2)$; ▲, $\text{Cp}_2\text{Nb}(\text{SiFMe}_2)(\text{H})(\text{SiXMe}_2)$; ×, $\text{Cp}_2\text{Nb}(\text{SiClMe}_2)(\text{H})(\text{SiXMe}_2)$; +, $\text{Cp}_2\text{Nb}(\text{SiBrMe}_2)(\text{H})(\text{SiXMe}_2)$; ●, $\text{Cp}_2\text{Nb}(\text{SiIme}_2)(\text{H})(\text{SiXMe}_2)$.

and Y, the larger the difference in chemical shifts of the SiXMe_2 and SiYMe_2 ligands is. Such a downfield shift is caused by an electronic rearrangement accompanying IHI. Namely, as IHI increases, more silicon s character is distributed to bonding to the pseudoequatorial substituents (the Nb and two Me groups on silicon),^{4a} causing an increase of the effective electronegativity of the silicon atom with respect to methyl groups. For this reason, the downfield Me shift correlates well with the contraction of the Nb–Si bonds observed in the Br and I families. The comparison of the same silyl groups in a series of related molecules provides the most convincing proof for the increase of IHI down the halogen group. For example, in the series $\text{Cp}_2\text{Nb}(\text{SiFMe}_2)(\text{H})(\text{SiXMe}_2)$, the SiFMe_2 group signal moves to lower field from 0.39 ppm for X = I to 0.52 ppm for X = F. Since both silyl groups are separated by the hydride, the magnetic environment of each SiFMe_2 group is the same (analogous anisotropy), and the difference in chemical shifts is related only to the different electronic effect of the SiXMe_2 groups. IHI in $\text{Cp}_2\text{Nb}(\text{SiFMe}_2)(\text{H})(\text{SiHMe}_2)$ (**2a**) is more localized on the $\text{H}\cdots\text{SiFMe}_2$ part; therefore, its SiFMe_2 group signal of 0.57 ppm is also downfield-shifted relative to the one in the symmetrical complex $\text{Cp}_2\text{Nb}(\text{SiFMe}_2)_2(\text{H})$ (0.52 ppm).

The dependence of the H–Si signal in complexes $\text{Cp}_2\text{Nb}(\text{SiXMe}_2)(\text{H})(\text{SiHMe}_2)$ on the nature of substituent X does not follow a simple electronegativity trend either (Figure 7). It is, however, hard to rationalize why compounds $\text{Cp}_2\text{Nb}(\text{SiFMe}_2)(\text{H})(\text{SiHMe}_2)$ (**2a**) and $\text{Cp}_2\text{Nb}(\text{SiHMe}_2)_2(\text{H})$ (**3**) with assumingly the strongest possible IHI of the type $\text{NbH}\cdots\text{SiHMe}_2$ have such downfield SiHMe_2 signals. It is also astonishing that the SiHMe_2 signal, unlike other NMR parameters, exhibits a maximum for the fluorine compound. Our tentative explanation is that, assuming that IHI $\text{NbH}\cdots\text{SiHMe}_2$ is weak if any, the inductive effect of the SiXMe_2 group starts to dominate. This is the strongest for X = F, so

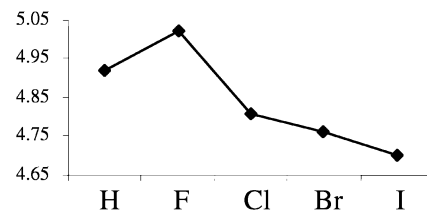


Figure 7. Dependence of the H–Si signal in complexes $\text{Cp}_2\text{Nb}(\text{SiXMe}_2)(\text{H})(\text{SiHMe}_2)$ on the nature of substituent X.

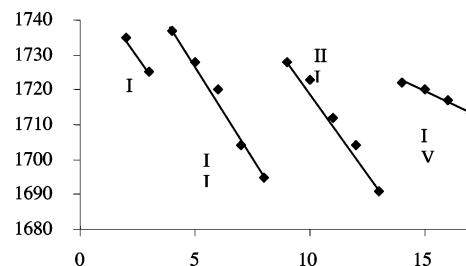


Figure 8. Dependence of the IR Nb–H stretch in complexes $\text{Cp}_2\text{Nb}(\text{SiXMe}_2)(\text{H})(\text{SiYMe}_2)$ on the nature of substituents X and Y. Group I: X = Y = OMe, SPh. Group II: X = H, Y = H, F, Cl, Br, I. Group III: X = F, Y = H, F, Cl, Br, I. Group IV: (X, Y) = (Cl, Cl), (Cl, Br), (Br, Br), (I, I).

that a superposition of two opposite effects of comparable magnitude (the inductive and IHI) can create an extremum.

Overall, the trends in the ^{13}C chemical shifts for the Cp and Me groups in $\text{Cp}_2\text{Nb}(\text{SiXMe}_2)(\text{H})(\text{SiYMe}_2)$ correlate well with the corresponding signals in the ^1H NMR spectra, although the ^{13}C signals exhibit a much decreased sensitivity. For example, for a given X, the SiXMe_2 signal remains almost constant regardless the variation of Y.

IR Studies. The most informative signals in the IR spectra of complexes $\text{Cp}_2\text{Nb}(\text{SiXMe}_2)(\text{H})(\text{SiYMe}_2)$ are the Si–H and Nb–H bands, found in the ranges of 1988–2006 cm^{-1} and 1690–1740 cm^{-1} , respectively (Figure 8). Classical bis(silyl) hydride $\text{Cp}_2\text{Nb}(\text{SiXMe}_2)_2(\text{H})$, without IHI, exhibits the Nb–H stretches at 1725–1735 cm^{-1} . Therefore, complexes with IHI show clear bathochromic shifts. A similar situation is found for other complexes with nonclassical Si–H interactions.⁶ For a given substituent X, the heavier halogens Y cause weaker Nb–H stretches. The most red-end bands are observed for compounds with the largest difference in the ability of X and Y to cause IHI (i.e., for X = H, F and Y = Br, I).

The Si–H stretches in $\text{Cp}_2\text{Nb}(\text{SiHMe}_2)(\text{H})(\text{SiXMe}_2)$ change irregularly, first increasing from X–H to X = Cl and then decreasing down Group 7. We have no rationale for this variation, although it is interesting to note that this trend is opposite to the variation of the Si–Nb–Si bond angle found by X-ray diffraction.

Conclusions

The intent of this research was to give an experimental verification of our earlier prediction that heavier halogen substituents at silicon atoms in halosilyl hydride derivatives of niobocene cause stronger interligand hypervalent interactions between the hydride and silyl ligands. We assumed that so far unknown asymmetric bis(silyl) complexes Cp_2Nb

Nb(SiYMe₂)(H)(SiXMe₂) would be an ideal object to check this hypothesis through the implementation of systematic structural studies. It was anticipated that differently substituted silyl groups will exhibit different structural distortions because of the *concurrent Si···H interligand interactions*. We have shown that selective functionalization of the Si–H bond in the precursor complex Cp₂Nb(SiHMe₂)₂(H) in most cases (except X = F) provides a convenient entry to the asymmetric complexes Cp₂Nb(SiHMe₂)(H)(SiXMe₂) which can be further converted into Cp₂Nb(SiYMe₂)(H)(SiXMe₂). Various halogenating reagents and conditions were tried. Although the selectivity of halogenation depends on both the electrophile and the solvent, the following generalizations can be made: (i) selectivity of H/F exchange increases in the sequence PF₅ < BF₃ < [CPh₃][BF₄] < [CPh₃][PF₆], (ii) selectivity of H/Cl exchange increases in the sequence SiCl₄ < PhNMe₂·HCl ≤ Me₃SnCl = PEt₂Cl, (iii) selectivity of H/Br exchange increases in the sequence Br₂·diox < PhNMe₂·HBr ≤ Me₃SnBr, and (iv) selectivity of H/I exchange increases in the sequence I₂ < MeI < Me₃SiI ≪ PhNMe₂·HI. The following effect of solvent was observed: hexane < toluene (benzene) < ether < THF. But the iodine-containing reagents react with ethereal solvents. Generally, these trends reflect the decreasing Lewis acidity and increased solvation or complexation of electrophiles by the solvent. The choice of reagent and solvent, however, is also determined by the reaction rate and the solubility and stability of the starting compounds and products (e.g., THF undergoes ring-opening by the SiMe₂I groups).

An unusual reactivity toward activated Si–H bonds and its surprising solvent dependence was encountered in reactions of trimethyl tin halides. Namely, the compound Cp₂Nb(SiHMe₂)₂(H) reacts with ISnMe₃ in toluene to give the product of *mono alkylation*, Cp₂Nb(SiMe₃)(H)(SiHMe₂), whereas a very similar reaction with ClSnMe₃ gives the product of *double alkylation*, Cp₂Nb(SiMe₃)₂(H). Both these aspects (the H/Me exchange instead of H/Hal metathesis and its selectivity) are very unusual and can be an interesting starting point for further investigations.

Although, most of the compounds prepared were characterized by X-ray diffraction, the analysis of systematic structural data was complicated by the X/Y disorder when the sizes of groups X and Y were comparable, namely, for Cp₂Nb(SiHMe₂)(H)(SiFMe₂), Cp₂Nb(SiClMe₂)(H)(SiBrMe₂), and Cp₂Nb(SiBrMe₂)(H)(SiIme₂). Nevertheless, the variation of key structural parameters (Nb–Si and Si–X bond lengths and the XSi–Nb–SiY bond angles) is in good agreement with the increase of IHI from X = Cl to X = I. Neutron diffraction studies of the compounds Cp₂Nb(SiHMe₂)(H)(SiClMe₂) and Cp₂Nb(SiHMe₂)(H)(SiBrMe₂), showing the hydride shift (by ~3°) to the SiBrMe₂ group in the latter complex, provide direct experimental proof for this conclusion. The fluorine substituent plays a special role among other halogens. Its shows almost the same structural parameters for the silyl group as a hydrogen substituent but, according to complementary DFT calculations by Lledos et al., causes a stronger FSi···HNb interaction than the IHI with the SiClMe₂ ligand.⁹ This deviation from the general trend is

most likely caused by the strong contribution of the electrostatic component in the FSi···HNb bonding. Unfortunately, our structural approach cannot underpin this component of interligand bonding.

Finally, systematic trends in the NMR and IR parameters provide further, although indirect, support for the strengthening of IHI down Group 7. The key observations are the upfield shift of the hydride resonance, the downfield shifts of the Cp and Me resonances in the ¹H NMR spectra and the red-end shifts of the Nb–H stretching bands in the IR spectra.

Experimental Section

All manipulations were carried out under anaerobic and anhydrous conditions. Solvents were dried over sodium or sodium benzophenone ketyl and distilled into the reaction vessel by high-vacuum gas-phase transfer. NMR spectra were recorded on Varian VXR-300 (¹H, 300 MHz; ¹³C, 100.4 MHz; ¹⁹F, 282.2 MHz). IR spectra were measured with a FTIR Perkin-Elmer 1600 series spectrometer as Nujol mulls. [Ph₃C][BF₄], [Ph₃C][PF₆], I₂, NaI (anhydrous), ClPEt₂, and ClSnMe₃ were purchased from Sigma-Aldrich. PhNMe₂, F₃B·Et₂O, and MeI were obtained from Merck and purified by distillation. ISiMe₃,²⁶ Br₂·diox,²⁷ ISnMe₃,²⁸ and Cp₂Nb(SiHMe₂)₂(H),^{4a} were prepared according to the literature. The preparation of [PhNHMe₂]₂X (X = Cl, Br, I) is given in Supporting Information.

Preparation of Cp₂Nb(SiFMe₂)(H)(SiHMe₂) (2a). A suspension of [Ph₃C][PF₆] (0.24 g, 0.626 mmol) in THF (10 mL) was added in portions to a solution of Cp₂Nb(SiHMe₂)₂(H) (0.64 g, 1.87 mmol) in THF (10 mL) at –40 °C. The reaction mixture became dark green. The mixture was stirred for 2 h, after which all volatiles were removed in vacuo. The residue was extracted twice by ether (2 × 10 mL); the solution was filtered, and volatiles were removed in vacuo. The compound was recrystallized twice by cooling hexane solutions to give white crystals of **2a** (0.18 g, 27%). IR (Nujol): ν(Nb–H) 1728, ν(Si–H) 1996 cm⁻¹. ¹H NMR (C₆D₆): δ –5.22 (s, 1 H, Nb–H), 0.43 (d, ³J_{H–H} = 3.8 Hz, 6 H, SiHMe₂), 0.57 (d, ³J_{H–F} = 7.6 Hz, 6 H, SiFMe₂), 4.45 (s, 10H, Cp), 5.02 (sept, ³J_{H–H} = 3.8 Hz, 1 H, Si–H). ¹³C NMR (C₆D₆): δ 5.5 (SiHMe₂), 8.5 (SiFMe₂), 89.3 (Cp). ¹⁹F NMR (C₆D₆): δ –122.8 (SiFMe₂). Anal. Calcd for C₁₄H₂₄FNbSi₂: C, 46.66; H, 6.71. Found: C, 46.79; H, 6.53.

Preparation of Cp₂Nb(SiClMe₂)(H)(SiHMe₂) (2b). A solution of trimethyltin chloride (1.82 g, 9.14 mmol) in ether (30 mL) was added to a solution of Cp₂Nb(SiHMe₂)₂(H) (3.13 g, 9.14 mmol) in ether (50 mL) at –40 °C. In 4 h, the solution was filtered, and all volatiles were removed in vacuo. The residue was washed twice by hexane (2 × 10 mL) and recrystallized from ether to give light beige crystals of **2b** (2.23 g, 65%). IR(Nujol): ν(Nb–H) 1720, ν(Si–H) 2006 cm⁻¹. ¹H NMR (C₆D₆): δ –4.58 (s, 1 H, Nb–H), 0.35 (d, ³J_{H–H} = 3.6 Hz, 6 H, SiHMe₂), 0.73 (s, 6 H, SiClMe₂), 4.52 (s, 10H, Cp), 4.81 (sept, ³J_{H–H} = 3.6 Hz, 1 H, Si–H). ¹³C NMR (C₆D₆): δ 5.1 (SiHMe₂), 13.9 (SiClMe₂), 91.1 (Cp). Anal. Calcd for C₁₄H₂₄ClNbSi₂: C, 44.62; H, 6.42. Found: C, 44.16; H, 6.47.

Preparation of Cp₂Nb(SiBrMe₂)(H)(SiHMe₂) (2c). To a solution of Cp₂Nb(SiHMe₂)₂(H) (1.10 g, 3.22 mmol) in 25 mL of

(26) Lissel, M. *Synthesis* **1983**, 6.

(27) Billimoria, J. D.; Maclagen, N. F. *J. Chem. Soc.* **1954**, 3257.

(28) Shishido K, Kinukawa J. Jpn. Patent 6626, 1955; *Chem. Abstr.* **1955**, 49, 9690.

toluene at $-40\text{ }^{\circ}\text{C}$ was added dropwise 11.3 mL of a solution of trimethyltin bromide (0.285 mmol/mL) in toluene. The reaction mixture was warmed to room temperature and stirred overnight, developing a dark-orange color. Volatiles were removed under reduced pressure, and the resultant light brown microcrystalline material was washed twice with ether ($2 \times 5\text{ mL}$) and dried in vacuum. Yield: 0.72 g (53%) of **2c**. IR (Nujol): $\nu(\text{Nb-H})$ 1704, $\nu(\text{Si-H})$ 2004 cm^{-1} . $^1\text{H NMR}$ (C_6D_6): δ -4.61 (s, 1 H, Nb-H), 0.33 (d, $^3J_{\text{H-H}} = 3.6\text{ Hz}$, 6 H, SiHMe_2), 0.87 (s, 6 H, SiBrMe_2), 4.53 (s, 10H, Cp), 4.77 (sept, $^3J_{\text{H-H}} = 3.6\text{ Hz}$, 1 H, Si-H). $^{13}\text{C NMR}$ (C_6D_6): δ 5.0 (SiHMe_2), 14.4 (SiBrMe_2), 91.8 (Cp). Anal. Calcd for $\text{C}_{14}\text{H}_{24}\text{BrNbSi}_2$: C, 39.91; H 5.74. Found: C, 39.47; H, 5.53.

Preparation of $\text{Cp}_2\text{Nb}(\text{SiMe}_2)(\text{H})(\text{SiHMe}_2)$ (2d**).** $\text{Cp}_2\text{Nb}(\text{SiHMe}_2)_2(\text{H})$ (0.94 g, 2.73 mmol) was added to a suspension of $[\text{PhNHMe}_2]\text{I}$ (0.68 g, 2.73 mmol) in 20 mL of ether. After 2 h of intensive stirring, a pink powder formed instead of the white ammonia salt. Gas evolution was observed in the course of the reaction. The precipitate was filtered, washed with cold ether (5 mL), and dried in vacuum to give 0.45 g (35%) of $\text{Cp}_2\text{Nb}(\text{SiMe}_2)(\text{H})(\text{SiHMe}_2)$ (pink powder). IR (Nujol): ν 1695 (Nb-H, w), 2000 cm^{-1} (Si-H, w). $^1\text{H NMR}$ (C_6D_6): δ -4.55 (s, 1 H, Nb-H), 0.29 (d, 6 H, SiHMe_2 , $^3J_{\text{HH}} = 4\text{ Hz}$), 1.04 (s, 6 H, SiMe_2), 4.53 (s, 10H, Cp), 4.70 (sept, 1 H, Si-H, $^3J_{\text{HH}} = 4\text{ Hz}$). $^{13}\text{C}\{^1\text{H}\}$ NMR (C_6D_6): δ 4.6 (s, SiHMe_2), 14.6 (s, SiMe_2), 92.7 (s, Cp). Anal. Calcd for $\text{C}_{14}\text{H}_{24}\text{INbSi}_2$: C, 35.91; H, 5.17. Found: C, 35.86; H, 5.21.

Reaction of $\text{Cp}_2\text{Nb}(\text{SiHMe}_2)_2(\text{H})$ with I_2 . A solution of I_2 (0.08 g, 0.3 mmol) in ether (10 mL) was added dropwise to a solution of $\text{Cp}_2\text{Nb}(\text{SiHMe}_2)_2(\text{H})$ (0.22 g, 0.64 mmol) in ether (10 mL), precooled to $-10\text{ }^{\circ}\text{C}$. Gas evolution was observed, and the initial dark red solution turned pink. The reaction mixture was stirred overnight, leading to the formation of a dark precipitate. The precipitate was filtered off and washed with ether ($3 \times 20\text{ mL}$). All volatiles were evaporated from the filtrate. The residue was washed with hexane and dried in vacuum to give a dark red solid (0.15 g) containing the starting material and the iodination products in a $\text{Cp}_2\text{Nb}(\text{SiHMe}_2)_2(\text{H})/\text{Cp}_2\text{Nb}(\text{SiMe}_2)(\text{H})(\text{SiHMe}_2)/\text{Cp}_2\text{Nb}(\text{SiMe}_2)_2(\text{H})$ ratio of 1:2:4 ($^1\text{H NMR}$). Some as yet unidentified products were observed by the $^1\text{H NMR}$ as well.

Reaction of $\text{Cp}_2\text{Nb}(\text{SiHMe}_2)_2(\text{H})$ with MeI. A. To a solution of $\text{Cp}_2\text{Nb}(\text{SiHMe}_2)_2(\text{H})$ (0.19 g, 0.55 mmol) in ether (20 mL) at $0\text{ }^{\circ}\text{C}$ was added a 0.8 M solution of MeI in ether (0.7 mL, 0.55 mmol). Vigorous evolution of a gas and the formation of a precipitate were observed. Analysis of the reaction mixture by $^1\text{H NMR}$ spectroscopy (C_6D_6) in 30 min revealed the absence of silyl-substituted niobocene complexes.

B. MeI (3 mL, 0.048 mmol) was added to a solution of $\text{Cp}_2\text{Nb}(\text{SiHMe}_2)_2(\text{H})$ (0.02 g, 0.05 mmol) in C_6D_6 (0.7 mL) in a NMR tube equipped with Teflon valve. The reaction was monitored by $^1\text{H NMR}$ spectroscopy. After a year at room temperature, the ratio of the starting material and the products, $\text{Cp}_2\text{Nb}(\text{SiHMe}_2)_2(\text{H})/\text{Cp}_2\text{Nb}(\text{SiMe}_2)(\text{H})(\text{SiHMe}_2)/\text{Cp}_2\text{Nb}(\text{SiMe}_2)_2(\text{H})$, was 7.5:1.5:1.

Reaction of $\text{Cp}_2\text{Nb}(\text{SiHMe}_2)_2(\text{H})$ with ISiMe_3 . A solution of $\text{Cp}_2\text{Nb}(\text{SiHMe}_2)_2(\text{H})$ (0.02 g, 0.05 mmol) and ISiMe_3 (6 μL , 0.05 mmol) in C_6D_6 (0.7 mL) was prepared in a sealed NMR tube. After 2 weeks at room temperature, the ratio of the starting material and products, $\text{Cp}_2\text{Nb}(\text{SiHMe}_2)_2(\text{H})/\text{Cp}_2\text{Nb}(\text{SiMe}_2)(\text{H})(\text{SiHMe}_2)/\text{Cp}_2\text{Nb}(\text{SiMe}_2)_2(\text{H})$, was found to be 6:3:1.

Reaction of $\text{Cp}_2\text{Nb}(\text{SiHMe}_2)_2(\text{H})$ with ISnMe_3 . $\text{Cp}_2\text{Nb}(\text{SiHMe}_2)_2(\text{H})$ (0.64 g, 1.8 mmol) was added to a 0.9 M solution of ISnMe_3 (2 mL, 1.8 mmol) in 30 mL of toluene frozen in liquid nitrogen. The red reaction mixture was warmed slowly (1 h) to room temperature and then stirred for 2 days. Analysis of the reaction

mixture by $^1\text{H NMR}$ showed the formation of $\text{Cp}_2\text{Nb}(\text{SiMe}_3)(\text{H})(\text{SiHMe}_2)$ (90%).

Preparation of $\text{Cp}_2\text{Nb}(\text{SiMe}_3)(\text{H})(\text{SiMe}_2)\text{H}$ (5**).** $[\text{PhNHMe}_2]\text{I}$ (0.42 g, 1.7 mmol) was added to 0.59 g (1.66 mmol) of $\text{Cp}_2\text{Nb}(\text{SiMe}_3)(\text{H})(\text{SiHMe}_2)$ in 30 mL of toluene, leading to evolution of a gas and gradual dissolving of the ammonium salt. In 3 h, all volatile components were removed in vacuo, and the red crystalline residue was washed with 10 mL of hexane. The yield is 0.45 g (56%). IR (Nujol): $\nu(\text{Nb-H})$ 1692 cm^{-1} . $^1\text{H NMR}$ (C_6D_6): δ -4.46 (s, 1 H, Nb-H), 0.19 (s, 9 H, SiMe_3), 1.04 (s, 6 H, SiMe_2), 4.54 (c, 10H, Cp). $^{13}\text{C NMR}$ (C_6D_6): δ 9.1 (SiMe_3), 14.9 (SiMe_2), 92.5 (Cp). Anal. Calcd for $\text{C}_{15}\text{H}_{26}\text{INbSi}_2$: C, 37.35; H, 5.43. Found: C, 37.06; H, 5.64.

Preparation of $\text{Cp}_2\text{Nb}(\text{SiFMe}_2)(\text{H})(\text{SiClMe}_2)$ (6**).** A suspension of $[\text{Ph}_3\text{C}][\text{BF}_4]$ (0.20 g, 0.61 mmol) in THF (10 mL) was added to a solution of $\text{Cp}_2\text{Nb}(\text{SiClMe}_2)(\text{H})(\text{SiHMe}_2)$ (0.23 g, 0.61 mmol) in THF (15 mL). In 20 min, the initially yellow solution became colorless. After it was stirred for 4 h, the reaction mixture was filtered off. All volatiles were removed under reduced pressure, and the residue was washed with hexane (10 mL). The product was dried in vacuum to give $\text{Cp}_2\text{Nb}(\text{SiFMe}_2)(\text{H})(\text{SiClMe}_2)$ (0.17 g, 73%) as colorless crystals. IR (Nujol): 1712 cm^{-1} (Nb-H, w). $^1\text{H NMR}$ (C_6D_6): δ -5.24 (s, 1 H, Nb-H), 0.44 (d, 6 H, SiFMe_2 , $^3J_{\text{HF}} = 8\text{ Hz}$), 0.68 (s, 6 H, SiClMe_2), 4.59 (s, 10H, Cp). $^{13}\text{C}\{^1\text{H}\}$ NMR (C_6D_6): δ 10.7 (d, SiFMe_2 , $^2J_{\text{CF}} = 14\text{ Hz}$), 13.7 (s, SiClMe_2), 90.7 (s, Cp). $^{19}\text{F}\{^1\text{H}\}$ NMR (C_6D_6): δ -124.7 . Anal. Calcd for $\text{C}_{14}\text{H}_{23}\text{ClFNBsi}_2$: C, 42.58; H, 5.87. Found: C, 42.27; H, 5.95.

Reaction of $\text{Cp}_2\text{Nb}(\text{SiClMe}_2)(\text{H})(\text{SiHMe}_2)$ with Excess $[\text{Ph}_3\text{C}][\text{BF}_4]$. $[\text{Ph}_3\text{C}][\text{BF}_4]$ (1 g, 3 mmol) was added to a solution of $\text{Cp}_2\text{Nb}(\text{SiClMe}_2)(\text{H})(\text{SiHMe}_2)$ (0.47 g, 1.25 mmol) in THF (20 mL). After the mixture was stirred for 4 h at room temperature, the analysis of the reaction mixture by $^1\text{H NMR}$ showed that the only niobocene-containing product was $\text{Cp}_2\text{Nb}(\text{SiFMe}_2)_2(\text{H})$.

Preparation of $\text{Cp}_2\text{Nb}(\text{SiFMe}_2)(\text{H})(\text{SiBrMe}_2)$ (7**).** A solution of $\text{F}_3\text{B}\cdot\text{Et}_2\text{O}$ (43 μL , 0.34 mmol) in THF (10 mL) was slowly added to a solution of $\text{Cp}_2\text{Nb}(\text{SiBrMe}_2)(\text{H})(\text{SiHMe}_2)$ (0.43 g, 1 mmol) in THF (20 mL) at $0\text{ }^{\circ}\text{C}$. After the mixture was stirred for 12 h, all volatiles were removed under reduced pressure, and the resulting solid residue was recrystallized from ether (20 mL) to give $\text{Cp}_2\text{Nb}(\text{SiFMe}_2)(\text{H})(\text{SiBrMe}_2)$ (0.32 g, 72%). IR (Nujol): 1704 cm^{-1} (Nb-H, w). $^1\text{H NMR}$ (C_6D_6): δ -5.25 (s, 1 H, Nb-H), 0.42 (d, 6 H, SiFMe_2 , $^3J_{\text{HF}} = 8\text{ Hz}$), 0.81 (s, 6 H, SiBrMe_2), 4.62 (s, 10H, Cp). $^{13}\text{C}\{^1\text{H}\}$ NMR (C_6D_6): δ 10.7 (d, SiFMe_2 , $^2J_{\text{CF}} = 14\text{ Hz}$), 14.1 (s, SiBrMe_2), 91.3 (s, Cp). $^{19}\text{F}\{^1\text{H}\}$ NMR (C_6D_6): δ -125.2 . Anal. Calcd for $\text{C}_{14}\text{H}_{23}\text{BrFNBsi}_2$: C, 38.28; H, 5.28. Found: C, 37.95; H, 5.05.

Reaction of $\text{Cp}_2\text{Nb}(\text{SiBrMe}_2)_2(\text{H})$ with $\text{F}_3\text{B}\cdot\text{Et}_2\text{O}$. To a solution of $\text{F}_3\text{B}\cdot\text{Et}_2\text{O}$ (50 μL , 0.4 mmol) in ether (30 mL) was added $\text{Cp}_2\text{Nb}(\text{SiBrMe}_2)_2(\text{H})$ (0.2 g, 0.4 mmol). Analysis of the reaction mixture by $^1\text{H NMR}$ spectroscopy after 3 d of stirring at room temperature showed the presence of the starting compound $\text{Cp}_2\text{Nb}(\text{SiBrMe}_2)_2(\text{H})$ and the product $\text{Cp}_2\text{Nb}(\text{SiFMe}_2)(\text{H})(\text{SiBrMe}_2)\text{H}$ in the 6:1 ratio.

Preparation of $\text{Cp}_2\text{Nb}(\text{SiFMe}_2)(\text{H})(\text{SiMe}_2)$ (8**).** $\text{F}_3\text{B}\cdot\text{Et}_2\text{O}$ (0.5 mL, 4.14 mmol) was added to a suspension of $\text{Cp}_2\text{Nb}(\text{SiMe}_2)_2(\text{H})$ (2.46 g, 4.14 mmol) in toluene (80 mL). The reaction mixture was stirred for 1 week at room temperature. The solid product was filtered off and washed twice with toluene (40 mL) (ultrasonic bath was used to homogenize the suspension before each filtration). All volatiles were removed under reduced pressure to give $\text{Cp}_2\text{Nb}(\text{SiFMe}_2)(\text{H})(\text{SiMe}_2)$ (0.7 g, 35%) as a pink powder. IR (Nujol): ν 1691 cm^{-1} (Nb-H, w). $^1\text{H NMR}$ (C_6D_6): δ -4.93 (s, 1 H, Nb-

H), 0.39 (d, 6 H, SiFMe₂, ³J_{HF} = 7 Hz), 0.99 (s, 6 H, SiMe₂), 4.61 (s, 10H, Cp). ¹³C{¹H} NMR (C₆D₆): δ 10.8 (d, SiFMe₂, ²J_{CF} = 13 Hz), 14.1 (s, SiMe₂), 91.3 (s, Cp). ¹⁹F{¹H} NMR (C₆D₆): δ -122.8. Anal. Calcd for C₁₄H₂₃FINbSi₂: C, 34.58; H, 4.77. Found: C, 34.40; H, 4.89.

Preparation of Cp₂Nb(SiFMe₂)(H)(Si(O(CH₂)₄I)Me₂) (9). F₃B·Et₂O (0.15 mL, 1.24 mmol) was added to a suspension of Cp₂Nb-(SiMe₂)₂(H) (2.2 g, 3.72 mol) in THF (70 mL), resulting in immediate dissolution of the precipitate. After the reaction mixture was stirred for 4 h at room temperature, all volatiles were removed under reduced pressure. The residue was washed with ether (20 mL) and dried in vacuum to give Cp₂Nb(SiFMe₂)(H)(Si(O(CH₂)₄I)-Me₂) (1.9 g, 91%). IR (Nujol): ν 1723 cm⁻¹ (Nb-H, w). ¹H NMR (C₆D₆): δ -4.88 (s, 1 H, Nb-H), 0.38 (s, 6 H, SiMe₂O), 0.56 (d, 6 H, SiFMe₂, ³J_{HF} = 8 Hz), 2.79 (m, 2H, OCH₂(CH₂)₃I), 2.86 (m, 2H, OCH₂CH₂(CH₂)₂I), 3.40 (m, 2H, O(CH₂)₂CH₂CH₂I), 3.64 (m, 2H, O(CH₂)₃CH₂I), 4.62 (s, 10H, Cp). ¹³C{¹H} NMR (C₆D₆): δ 6.4 (s, CH₂), 9.0 (s, SiMe₂O), 10.8 (d, SiFMe₂, ²J_{CF} = 13 Hz), 30.4 (s, CH₂), 32.5 (s, CH₂), 64.5 (s, OCH₂), 88.9 (s, Cp). ¹⁹F{¹H} NMR (C₆D₆): δ -123.8. Anal. Calcd for C₁₈H₃₁FINbOSi₂: C, 38.72; H, 5.60. Found: C, 38.61; H, 5.42.

Reaction of Cp₂Nb(SiFMe₂)(H)(SiClMe₂) with ISiMe₃. ISiMe₃ (1 mL, 7 mmol) was added to a solution of Cp₂Nb(SiFMe₂)(H)-(SiClMe₂) (0.12 g, 0.3 mmol) in ether (10 mL). The initially colorless solution turned dark red, and a dark solid formed. Analysis of the reaction mixture by ¹H NMR spectroscopy, after it was stirred for 30 min, showed no signals of silylniobocene complexes (both in C₆D₆ and CDCl₃ solutions).

Preparation of Cp₂Nb(SiClMe₂)(H)(SiBrMe₂) (10). Method I. CIPe_t (0.13 mL, 1.3 mmol) was added to a suspension of Cp₂Nb(SiBrMe₂)(H)(SiHMe₂) (0.58 g, 1.34 mmol) in ether (20 mL). The reaction mixture was stirred overnight to give a yellow precipitate, which was filtered off and washed with ether (3·20 mL). The combined filtrates were evaporated under reduced pressure to give Cp₂Nb(SiClMe₂)(H)(SiBrMe₂) (0.55 g, 90%) as a yellow powder.

Method II. Cp₂Nb(SiBrMe₂)(H)(SiHMe₂) (0.49 g, 1.16 mmol) was added to a solution of [PhNHMe₂]Cl (0.17 g, 1.1 mmol) in THF (80 mL) frozen in liquid nitrogen. The reaction mixture was slowly (3 h) warmed to ambient temperature; evolution of a gas was observed. The reaction mixture was stirred overnight, and then all volatiles were removed under reduced pressure. The solid residue thus obtained was washed with cold ether (10 mL) to give Cp₂Nb(SiClMe₂)(H)(SiBrMe₂) (0.45 g, 85%) as a beige powder.

Method III. Cp₂Nb(SiClMe₂)(H)(SiHMe₂) (0.29 g, 0.78 mmol) was added to a solution of [PhNHMe₂]Br (0.15 g, 0.74 mmol) in THF (50 mL) frozen in liquid nitrogen. The reaction mixture was slowly (3 h) warmed up to ambient temperature, and evolution of a gas was observed. The reaction mixture was stirred overnight, and then all volatiles were removed under reduced pressure. The solid residue was washed with cold ether (3 mL) to give Cp₂Nb(SiClMe₂)(H)(SiBrMe₂) (0.12 g, 34%) as a beige powder.

IR (Nujol): ν 1720 cm⁻¹ (Nb-H, w). ¹H NMR (C₆D₆): δ -5.17 (s, 1H, Nb-H), 0.57 (s, 6H, SiClMe₂), 0.73 (s, 6H, SiBrMe₂), 4.67 (s, 10H, Cp). ¹³C{¹H} NMR (C₆D₆): δ 13.6 (s, SiClMe₂), 14.1 (s, SiBrMe₂), 93.0 (s, Cp). Anal. Calcd for C₁₄H₂₃BrClNbSi₂: C, 36.89; H, 5.09. Found: C, 36.54; H, 5.15.

Reaction of Cp₂Nb(SiClMe₂)(H)(SiHMe₂) with Br₂·dioxane. A solution of Br₂·dioxane (0.08 g, 0.32 mmol) in ether (20 mL) was added to a solution of Cp₂Nb(SiClMe₂)(H)(SiHMe₂) (0.23 g, 0.63 mmol) in ether (20 mL), cooled down to 0 °C. The reaction mixture was stirred overnight. Analysis by ¹H NMR spectroscopy of the pink solution over the beige precipitate showed the formation

of a statistical mixture of chloro and bromo, mono- and bis(halo)-substituted bis(silyl) niobocenes.

Reaction of Cp₂Nb(SiBrMe₂)(H)(SiHMe₂) with ClSnMe₃. ClSnMe₃ (0.13 g, 0.66 mmol) was added to a solution of Cp₂Nb-(SiBrMe₂)(H)(SiHMe₂) (0.28 g, 0.66 mmol) in toluene (30 mL) frozen in liquid nitrogen. The reaction mixture was slowly (6 h) warmed to ambient temperature, and it was then stirred for 3 days. Analysis of the reaction mixture by ¹H NMR spectroscopy showed the formation of Cp₂Nb(SiClMe₂)(H)(SiHMe₂) as the only niobocene-containing product. All volatiles were removed under reduced pressure to give Cp₂Nb(SiClMe₂)(H)(SiHMe₂) (0.24 g, 96%).

Reaction of Cp₂Nb(SiBrMe₂)(H)(SiHMe₂) with Cl₄Si. Cp₂Nb-(SiBrMe₂)(H)(SiHMe₂) (0.57 g, 1.4 mmol) was added to a solution of SiCl₄ (1.62 mL, 14.1 mmol) in ether (20 mL) frozen in liquid nitrogen. The reaction mixture was slowly (3 h) warmed to ambient temperature. Analysis of the reaction mixture, after 4 h of stirring, by ¹H NMR spectroscopy showed the presence of starting complex Cp₂Nb(SiBrMe₂)(H)(SiHMe₂) and the only product Cp₂Nb(SiClMe₂)₂(H) in a ratio of 9:1.

Preparation of Cp₂Nb(SiClMe₂)(H)(SiMe₂) (11). Cp₂Nb-(SiClMe₂)(H)(SiHMe₂) (0.11 g, 0.3 mmol) was added to a suspension of [PhNHMe₂]I (0.07 g, 0.28 mmol) in ether (20 mL) frozen in liquid nitrogen. The reaction mixture was slowly (3 h) warmed to ambient temperature, and then, it was stirred for additional 4 h. Analysis of the reaction mixture by ¹H NMR spectroscopy showed the presence of starting complex Cp₂Nb(SiClMe₂)(H)(SiHMe₂) and the products Cp₂Nb(SiClMe₂)(H)(SiMe₂) and Cp₂Nb(SiClMe₂)₂(H) in an approximate ratio of 1:1:1. All volatiles were removed under reduced pressure, and the solid residue was washed with ether (4 mL) to leave the less-soluble Cp₂Nb(SiClMe₂)(H)(SiMe₂) (0.04 g, 29%). ¹H NMR (C₆D₆): δ -5.06 (s, 1 H, Nb-H), 0.55 (s, 6 H, SiClMe₂), 0.92 (s, 6 H, SiMe₂), 4.68 (s, 10H, Cp). ¹³C{¹H} NMR (C₆D₆): δ 13.7 (SiClMe₂), 14.6 (SiMe₂), 94.1 (Cp). Anal. Calcd for C₁₄H₂₃ClINbSi₂: C, 33.44; H, 4.61. Found: C, 32.76; H, 3.97.

Reaction of Cp₂Nb(SiBrMe₂)(H)(SiHMe₂) with I₂. A solution of I₂ (0.2 g, 0.78 mmol) in ether (10 mL) was slowly added to a solution of Cp₂Nb(SiBrMe₂)(H)(SiHMe₂) (0.65 g, 1.54 mmol) in ether (20 mL), precooled to -10° C. Gas evolution was observed, and the color of the solution changed from dark red to light red in 1 h. The reaction mixture was stirred overnight. The solid product was filtered off and washed with ether (2 × 10 mL). Volatiles were removed from combined fractions under reduced pressure to give a mixture (0.42 g) of Cp₂Nb(SiBrMe₂)(H)(SiMe₂) (12), Cp₂Nb-(SiBrMe₂)₂(H), and Cp₂Nb(SiMe₂)₂(H) in a ratio of 6:2:1.

Cp₂Nb(SiBrMe₂)(H)(SiMe₂). ¹H NMR (C₆D₆): δ -4.55 (s, 1 H, Nb-H), 0.30 (s, 6 H, SiBrMe₂), 1.04 (s, 6 H, SiMe₂), 4.70 (s, 10H, Cp). ¹³C NMR (C₆D₆): δ 14.2 (SiBrMe₂), 14.6 (SiMe₂), 94.7 (Cp). Anal. Calcd for C₁₄H₂₃BrINbSi₂: C 30.73, H 4.24; Found: C 29.95, H 4.36

X-ray Diffraction Studies. Crystal Structure Determinations. Light-brown crystals of Cp₂Nb(SiHMe₂)(H)(SiFMe₂) (2a), colorless crystals of Cp₂Nb(SiHMe₂)(H)(SiClMe₂) (2b), light-beige crystals of Cp₂Nb(SiHMe₂)(H)(SiBrMe₂) (2c), pink crystals of Cp₂Nb-(SiHMe₂)(H)(SiMe₂) (2d), pink crystals of Cp₂Nb(SiMe₃)(H)-(SiMe₂) (5d), colorless crystals of Cp₂Nb(SiFMe₂)(H)(SiClMe₂) (6), light-brown crystals of Cp₂Nb(SiFMe₂)(H)(SiBrMe₂) (7), violet crystals of Cp₂Nb(SiMe₂)(H)(SiBrMe₂) (12), and light-brown crystals of Cp₂Nb(SiClMe₂)(H)(SiBrMe₂) (9) were grown from ether by cooling the solutions to -25 to -30 °C. Purple crystals of Cp₂Nb(SiFMe₂)(H)(SiMe₂) (8) were grown from toluene by cooling the solution to -20 °C.

A single crystal of each of these compounds was covered with polyperfluorinated oil and mounted on a Bruker SMART CCD

Table 4. Crystal Data, Data Collection, Structure Solution, and Refinement Parameters for X-ray Investigations

	2a	2b	2c	2d	5d
formula	C ₁₄ H ₂₄ FNbSi ₂	C ₁₄ H ₂₄ ClNbSi ₂	C ₁₄ H ₂₄ BrNbSi ₂	C ₁₄ H ₂₄ INbSi ₂	C ₁₅ H ₂₆ INbSi ₂
fw	360.42	376.87	421.33	468.32	482.35
cryst syst	orthorhombic	monoclinic	monoclinic	monoclinic	monoclinic
space group	<i>P</i> 2 ₁ 2 ₁ 2 ₁	<i>P</i> 2 ₁ / <i>c</i>	<i>C</i> 2/ <i>c</i>	<i>C</i> 2/ <i>c</i>	<i>P</i> 2 ₁ / <i>c</i>
unit cell dimensions	<i>a</i> = 7.9990(3) Å, <i>α</i> = 90° <i>b</i> = 23.0146(8) Å, <i>β</i> = 90° <i>c</i> = 8.7090(3) Å, <i>γ</i> = 90°	<i>a</i> = 13.6876(4) Å, <i>α</i> = 90° <i>b</i> = 8.5767(3) Å, <i>β</i> = 93.627(2)° <i>c</i> = 14.5354(4) Å, <i>γ</i> = 90°	<i>a</i> = 14.9449(5) Å, <i>α</i> = 90° <i>b</i> = 8.9330(3) Å, <i>β</i> = 99.408(2)° <i>c</i> = 26.0528(9) Å, <i>γ</i> = 90°	<i>a</i> = 15.0574(10) Å, <i>α</i> = 90° <i>b</i> = 8.9249(5) Å, <i>β</i> = 98.113(2)° <i>c</i> = 26.0929(18) Å, <i>γ</i> = 90°	<i>a</i> = 13.7575(4) Å, <i>α</i> = 90° <i>b</i> = 8.2799(2) Å, <i>β</i> = 101.7380(10)° <i>c</i> = 16.7677(5) Å, <i>γ</i> = 90°
<i>V</i> (Å ³)	1603.3(1)	1702.96(9)	3431.3(2)	3471.4(4)	1870.08(9)
<i>Z</i>	4	4	8	8	4
<i>d</i> _{calcd} (g cm ⁻³)	1.493	1.470	1.631	1.792	1.713
abs coeff (mm ⁻¹)	0.893	0.987	3.154	2.594	2.410
<i>F</i> (000)	744	776	1928	1840	952
<i>θ</i> range (deg)	1.77–27.50	1.49–27.00	1.58–27.00	2.66–28.50	2.48–29.00
reflns collected	11 302	10 937	12 752	8089	11 895
independent reflns [<i>R</i> _{int}]	3683 [0.044]	3709 [0.0356]	3749 [0.0819]	4043 [0.0245]	4806 [0.0222]
data/params	3683/265	3709/245	3749/167	4043/259	4806/277
GOF on <i>F</i> ²	1.053	1.155	1.280	1.004	1.036
<i>R</i> 1 [<i>I</i> > 2σ(<i>I</i>)]	0.0262	0.0247	0.0650	0.025	0.0240
w <i>R</i> 2 (all data)	0.0653	0.0691	0.1649	0.0703	0.0547
largest diff peak/hole (e Å ⁻³)	0.569/−0.426	0.584/−0.591	1.853/0.000	1.079/−0.699	0.681/−0.787

	6	7	8	10	12
formula	C ₁₄ H ₂₃ ClFNbSi ₂	C ₁₄ H ₂₃ BrFNbSi ₂	C ₁₄ H ₂₃ FINbSi ₂	C ₁₄ H ₂₃ BrClINbSi ₂	C ₁₄ H ₂₃ BrINbSi ₂
fw	394.86	444.20	485.31	455.77	547.22
cryst syst	monoclinic	monoclinic	monoclinic	orthorhombic	orthorhombic
space group	<i>C</i> 2/ <i>c</i>	<i>C</i> 2/ <i>c</i>	<i>C</i> 2/ <i>c</i>	<i>P</i> <i>n</i> <i>m</i> <i>a</i>	<i>P</i> <i>b</i> <i>n</i> <i>m</i>
unit cell dimensions	<i>a</i> = 14.6577(5) Å, <i>α</i> = 90° <i>b</i> = 9.0181(3) Å, <i>β</i> = 99.760(1)°, <i>c</i> = 25.8731(9) Å, <i>γ</i> = 90°	<i>a</i> = 14.9940(4) Å, <i>α</i> = 90° <i>b</i> = 8.9459(2) Å, <i>β</i> = 99.3870(10)° <i>c</i> = 25.9221(7) Å, <i>γ</i> = 90°	<i>a</i> = 15.1427(10) Å, <i>α</i> = 90° <i>b</i> = 8.9369(10) Å, <i>β</i> = 98.304(2)° <i>c</i> = 26.143(2) Å, <i>γ</i> = 90°	<i>a</i> = 16.6006(5) Å, <i>α</i> = 90° <i>b</i> = 13.1582(4) Å, <i>β</i> = 90° <i>c</i> = 8.4922(2) Å, <i>γ</i> = 90°	<i>a</i> = 8.6829(2) Å, <i>α</i> = 90° <i>b</i> = 16.9020(4) Å, <i>β</i> = 90° <i>c</i> = 13.1647(2) Å, <i>γ</i> = 90°
<i>V</i> (Å ³)	1677.6(3)	3430.50(15)	3500.8(5)	1854.99(9)	1932.03(7)
<i>Z</i>	8	8	8	4	4
<i>d</i> _{calcd} (g cm ⁻³)	1.556	1.720	1.842	1.632	1.881
abs coeff (mm ⁻¹)	1.010	3.352	2.584	3.063	4.401
<i>F</i> (000)	1616	1777	1896	912	1056
<i>θ</i> range (deg)	2.66–28.99	1.59–27.00	1.57–27.51	2.45–29.00	2.41–27.00
reflns collected	11 019	11 871	10 487	12 244	12 403
independent reflns [<i>R</i> _{int}]	4288 [0.037]	4145 [0.0491]	3966 [0.0278]	2568 [0.0241]	2198 [0.0472]
data/params	4288/264	4145/262	3966/176	2568/150	2198/140
GOF on <i>F</i> ²	1.058	1.065	1.029	1.029	1.086
<i>R</i> 1 [<i>I</i> > 2σ(<i>I</i>)]	0.0547	0.0442	0.0292	0.0176	0.0231
w <i>R</i> 2 (all data)	0.0727	0.1095	0.0719	0.0419	0.0534
largest diff peak/hole (e Å ⁻³)	0.590/−0.515	2.27/−1.35	1.552/−0.473	0.408/−0.357	0.559/−0.549

diffractometer. Experimental data were measured using graphite-monochromatized Mo K α radiation ($\lambda = 0.71073$ Å) in ω -scan mode with steps of 0.3°. The crystallographic data and characteristics of structure solution and refinement are listed in Table 4. The Bruker SAINT program²⁹ was used for data reduction. An absorption correction based on measurements of equivalent reflections (SADABS³⁰) was applied. The structures were solved by direct methods³¹ and refined by full-matrix least-squares on *F*² with anisotropic thermal parameters for all non-hydrogen atoms (unless otherwise specified).³⁰ In **5d**, **6–8**, **10**, and **12**, all H atoms were found from difference Fourier synthesis and refined isotropically. The details of specific compounds are given in Supporting Information.

Neutron Diffraction Study of 2b. In an inert atmosphere chamber, a dark gray platelike crystal with dimensions of 2 × 2 ×

0.4 mm³ was covered with fluorinated grease, wrapped in aluminum foil, glued, and mounted onto an aluminum pin. The crystal was cooled to 100 K with a Displex closed-cycle helium refrigerator (Air Products and Chemicals, Inc., Model CS-202).³² Single-crystal neutron data of the title compound were collected on the single-crystal diffractometer (SCD) at the Intense Pulse Neutron Source (IPNS) of Argonne National Laboratory. An auto-indexing routine was used to obtain an orientation matrix.³³ The large number of parameters in the structure and the small sample size required the use of combined X-ray/neutron data in the structure analysis. Because of the small size of the crystal for neutron diffraction, the neutron data were measured at the same temperature (100 K) as the X-ray data to allow a combined refinement using GSAS,³⁴ a program commonly used for the joint X-ray/neutron refinement of powder and single-crystal diffraction data. In this type of refinement, because of the differences in the form factors for neutrons and X-rays, the parameters of the non-hydrogen atoms are essentially

(29) SAINT, version 6.02A; Bruker AXS Inc.: Madison, WI, 2001.

(30) Sheldrick, G. M. SADABS, Program for scaling and correction of area detector data; University of Göttingen: Göttingen, Germany, 1997.

(31) SHELXTL, release 5.10; Bruker AXS Inc.: Madison, WI, 1997.

(32) Schultz, A. J.; Srinivasan, K.; Teller, R. G.; Williams, J. M.; Lukehart, C. M. *J. Am. Chem. Soc.* **1984**, *106*, 999.

(33) Jacobson, R. A. *J. Appl. Crystallogr.* **1986**, *19*, 283.

Table 5. Crystal Data, Data Collection, Structure Solution, and Refinement Parameters for Neutron Diffraction Investigations of **2b** and **2c**

	2b	2c
formula	C ₁₄ H ₂₄ ClNbSi ₂	C ₁₄ H ₂₄ BrNbSi ₂
fw	376.87	421.33
temp (K)	100	83
cryst size (mm ³)	2 × 2 × 0.4	2 × 2 × 1
cryst syst	monoclinic	monoclinic
space group	<i>P2₁/c</i>	<i>C2/c</i>
unit cell dimensions	<i>a</i> = 13.6876(4) Å, <i>α</i> = 90° <i>b</i> = 8.5767(3) Å, <i>β</i> = 93.627(2)° <i>c</i> = 14.5354(4) Å, <i>γ</i> = 90°	<i>a</i> = 14.9449(5) Å, <i>α</i> = 90° <i>b</i> = 8.9330(3) Å, <i>β</i> = 99.408(2)° <i>c</i> = 26.0528(9) Å, <i>γ</i> = 90°
<i>V</i> (Å ³)	1702.96(9)	3431.3(2)
<i>Z</i>	4	8
<i>R</i> (F)	0.027 ^a	
<i>R</i> (wF)	0.034 ^a	
<i>R</i> (F)	0.112 ^b	0.1186
<i>R</i> (wF)	0.082 ^b	0.2678

^a Combined X-ray data; 4109 reflections. ^b Neutron data; 826 reflections.

determined by the X-ray data and the parameters of the hydrogen atoms are determined by the neutron data. Data collection and refinement parameters are summarized in Table 5, and selected distances and angles are given in Table 1. The final agreement factors (for all data) are *R*(wF) = 0.034, *R*(F) = 0.027, and GOF = 1.43 for the combined X-ray/neutron data set (4109 reflections) and *R*(wF) = 0.082 and *R*(F) = 0.112 for the 826 neutron reflections.

Neutron Diffraction Study of 2c. Data were collected on a dark gray prismatic crystal with approximate dimensions of 2.0 × 2.0 × 1.0 mm³ using the four-circle diffractometer D19 instrument (Institut Laue-Langevin in Grenoble, France), equipped with a Displex cryostat³⁵ and a curved position-sensitive area detector. A new flat “square” (192 × 192 mm) position-sensitive microstrip

detector has recently been added to the original curved detector.³⁶ Bragg intensities were integrated using the program Retreat,³⁷ and the structure was refined using SHELXTL.³¹ A total of 3282 reflections were used for full-matrix least-squares refinement. Data collection and refinement parameters are summarized in Table 5, and selected distances and angles are given in Table 1. The final agreement factors (for *I* > 2σ) are *R*(wF) = 0.2678, *R*(F) = 0.1186, and GOF = 1.747 (2271 reflections).

Acknowledgment. The ND study was supported by U.S. National Science Foundation (Grant CHE-98-16294) and NASA Grant CRG-921317. Work at Argonne was supported by the U.S. Department of Energy, Basic Energy Sciences, Materials Science, under Contract W-31-109-ENG-38. G.I.N. is grateful to the Russian Foundation for Basic Research (RFBR, Grant 00-03-32850) and Brock University (new faculty research grant) for financial support. Additional support from the RFBR to L.G.K. (Grant 01-03-32474) is gratefully acknowledged. L.G.K. and J.A.K.H. also thank the Royal Society (London) of Chemistry for a Joint Research Grant.

Supporting Information Available: X-ray data (CIF) for **2a–d**, **5d**, **6–8**, **10**, and **12**, figures for molecular structures of **2a–c**, **7**, **8**, **10**, and **12**, details for X-ray and ND analyses, and supplementary data for spectroscopic characterization of complexes Cp₂Nb(SiXMe₂)(H)(SiYMe₂). This material is available free of charge via the Internet at <http://pubs.acs.org>.

IC061314B

- (34) Larson, A. C.; Von Dreele, R. B. *GSAS: General Structure Analysis System*; Los Alamos National Laboratory: Los Alamos, NM, 1994.
- (35) Thomas, M.; Stansfield, R. F. D.; Berneron, M.; Filhol, A.; Greenwood, G.; Jacobe, J.; Feltin, D.; Mason, S. A. *Position-Sensitive Detection of Thermal Neutrons*; Convert, P., Forsyth, J. B., Eds; Academic Press: London, U.K., 1983; p 344.
- (36) Archer, J.; Lehmann, M. S. *J. Appl. Crystallogr.* **1986**, *19*, 456.
- (37) Wilkinson, C.; Khamis, H. W.; Stansfield, R. F. D.; McIntyre, G. J. *J. Appl. Crystallogr.* **1988**, *21*, 471